

Journal Pre-proof

Highly efficient one pot palladium-catalyzed synthesis of 3,5-bis (arylated) pyridines:
Comparative experimental and DFT studies

Muhammad Akram, Muhammad Adeel, Muhammad Khalid, Muhammad Nawaz Tahir,
Hossein Asghar Rahnamaye Aliabad, Malik Aman Ullah, Javed Iqbal, Atualpa A.C.
Braga

PII: S0022-2860(20)30456-7

DOI: <https://doi.org/10.1016/j.molstruc.2020.128131>

Reference: MOLSTR 128131

To appear in: *Journal of Molecular Structure*

Received Date: 15 October 2019

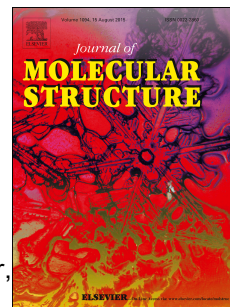
Revised Date: 23 March 2020

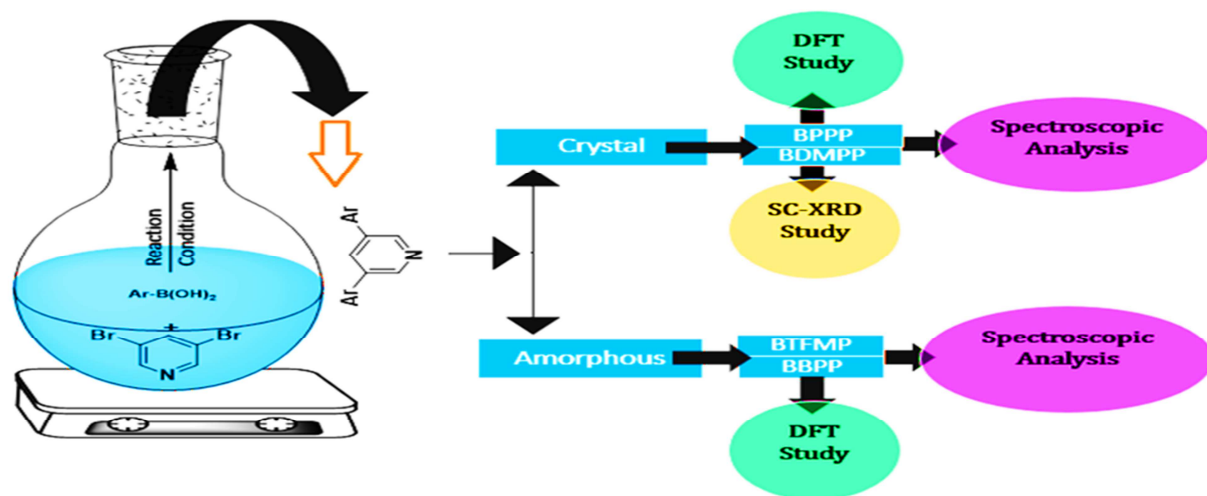
Accepted Date: 23 March 2020

Please cite this article as: M. Akram, M. Adeel, M. Khalid, M.N. Tahir, H.A.R. Aliabad, M.A. Ullah, J. Iqbal, A.A.C. Braga, Highly efficient one pot palladium-catalyzed synthesis of 3,5-bis (arylated) pyridines: Comparative experimental and DFT studies, *Journal of Molecular Structure* (2020), doi: <https://doi.org/10.1016/j.molstruc.2020.128131>.

This is a PDF file of an article that has undergone enhancements after acceptance, such as the addition of a cover page and metadata, and formatting for readability, but it is not yet the definitive version of record. This version will undergo additional copyediting, typesetting and review before it is published in its final form, but we are providing this version to give early visibility of the article. Please note that, during the production process, errors may be discovered which could affect the content, and all legal disclaimers that apply to the journal pertain.

© 2020 Published by Elsevier B.V.





Highly Efficient one Pot Palladium-Catalyzed Synthesis of 3,5-bis (arylated) pyridines: Comparative Experimental and DFT Studies

Muhammad Akram^{b,c}, Muhammad Adeel*^a, Muhammad Khalid*^d, Muhammad Nawaz Tahir^e, Hossein Asghar Rahnamaye Aliabad^f, Malik Aman Ullah^a, Javed Iqbal^g, Ataulpa A. C.Braga^h

^a Institute of Chemical Sciences, Gomal University, Dera Ismail Khan, Khyber Pukhtoonkhwa, Pakistan

^b Medicinal Botanic Centre, PCSIR Laboratories Complex Peshawar, Khyber Pukhtoonkhwa, Pakistan

^c Institute of Chemical Sciences, University of Peshawar, Peshawar, Khyber Pukhtoonkhwa, Pakistan

^d Department of Chemistry, Khwaja Fareed University of Engineering & Information Technology, *Rahim Yar Khan-64200, Pakistan*

^e Department of Physics, University of Sargodha, Sargodha, Punjab, Pakistan

^f Department of Physics, Hakim Sabzevari University, Sabzevar, 96179-76487, Iran

^g Department of Chemistry, University of Agriculture, Faisalabad-38000, Pakistan

^h Departamento de Química Fundamental, Instituto de Química, Universidade de São Paulo, Av. Prof. Lineu Prestes, 748, São Paulo, 05508-000, Brazil.

* Corresponding authors E-mail addresses:

(Dr. Muhammad Adeel) madeel@gu.edu.pk

(Dr. Muhammad Khalid) khalid@iq.usp.br; muhammad.khalid@kfueit.edu.pk

Abstract

Many different alkyl and aryl substituted pyridine based organic derivatives have been synthesized due to its uniqueness pyridine core. However, the transition metal catalyzed Suzuki cross coupling reaction has provided an easy route to the synthesis of alkyl and aryl substituted pyridine based organic compounds. Herein, we reported the arylated pyridines derivatives: 3, 5-bis (4-(trifluoromethoxy) phenyl) pyridine (**BTFMP**), 3,5-bis(4-bromophenyl)pyridine(**BBPP**), 3,5-bis(4-phenoxyphenyl)pyridine (**BPPP**) and 3,5-bis(2,5-dimethoxyphenyl)pyridine (**BDMPP**) by cross coupling Suzuki methodology for the first time. All derivatives have been characterized through ¹H NMR, ¹³CNMR, ¹⁹F NMR and FT-IR spectroscopic techniques. Two compounds (**BPPP**) and (**BDMPP**) exist in the form of crystals among studied compounds. Therefore, SC-XRD has been performed for **BPPP** and **BDMPP**. In addition, computational studies using density functional theory (DFT) have been carried out in order to compare the DFT based data with the experimental findings. The optimization, FT-IR, natural bond orbitals (NBOs), frontier

molecular orbitals (FMOs) and nonlinear optical (NLO) calculations of all derivatives have been performed using B3LYP/6-311G(d,p) level. The simulated HOMO-LUMO energy difference is observed to be large which shows the kinetic stability of the molecules. The molecular stability also originating from charge delocalization and hyper conjugative interactions has been elucidated by NBO analysis. MEP surfaces are also developed of entitled molecules. The NLO data pointed out that the first order hyperpolarizability for **BTFMP**, **BBPP** and **BPPP** is greater among studied molecules than the standard molecule.

Introduction:

Diversified biological activities and electronic properties make pyridine ring as unique structural motif. Due to its uniqueness pyridine core has found numerous applications in pharmaceutical science[1], agriculture[2], material science[3], catalysis[4] and organometallic chemistry[5]. Arylated pyridines have found multiple applications as building blocks for numerous pharmaceuticals, ligands for organic synthesis and in material science as organic materials[6]. Starting with 2-chloro-3-hydroxypyridine, Schmitt and co-workers for the first time had synthesized pentaarylpyridine having five different aryl groups[7]. Use of zinc metal in cross-coupling Suzuki reaction resulting in structural variations regarding alkyl, aryl and alkynyl groups in substituted pyridines have been achieved by treating respective halides with boronic acids [8]. Easily achievable reaction conditions and availability of modern spectroscopic methods of structure elucidation has made preparation of these compounds via C-C bond formation very easy route to increase data base of organic compounds. Riser reaction is other synthetically useful process which has employed for the synthesis of sulfur containing pyridine derivatives [9].

The preparation and microtubule destabilizing properties of pyridine chalcone derivatives have been designed and biological studies performed[10]. Palladium having the property of being easily oxidized and reduced has found most frequent use of palladium (II) complexes as catalysts in the preparation of compounds extending C-C bonds formation [11]. A high regioselectivity control has been observed in preparing pyridine derivatives applying Suzuki-Moriyama synthesis [12]. Moreover, pyridine has been widely used in Knoevenagel in the extension of carbon-carbon bonds in many reactions [13]. Brominated bishamides contain both electrons donating and withdrawing groups have been prepared and used in Suzuki coupling to obtain in excellent yield[14]. Asako et al. (2017) has reported the preparation of multiply-arylated pyridines by

cross-coupling reaction of hydroxylaryl pyridines with bromine containing compounds [15]. Valuable novel Pyridines containing dihydroferrocenyl group have been reported [16]. Many differently substituted pyridines derivatives have been prepared. Their photophysical properties have been investigated and DFT studies of the complexes prepared from prepared pyridines containing intermediates as a function of different substituent have reported [17]. Transition metal catalyzed Suzuki cross coupling reaction has provided an easy route to the synthesis of alkyl and aryl substituted pyridine based organic compounds. The Palladium (Pd) metal being easily oxidized and reduced is most commonly used metal for cross coupling Suzuki reaction to synthesize many compounds of medicinal interest [18]. We have already reported some studies on arylated pyridines [19]. Now in order to expand our knowledge on arylated pyridines, herein we report synthesis, single crystal XRD and DFT of studies of novel arylated pyridines; which are never reported in literature to the best of our knowledge.

Experimental

Material and method

IR spectra were recorded from Bruker Alpha FT-IR spectrometer. Melting points were recorded on Fisher-John melting point apparatus. Bruker NMR spectrometers were used to get NMR spectra working on 500 MHz and 400 MHz, 125 MHz and 75 MHz and 470 MHz for ^1H NMR, ^{13}C NMR and ^{19}F NMR respectively, using TMS as internal standard.

Synthetic procedure and characterization

3, 5-bis (4-(trifluoromethoxy) phenyl) pyridine (BTFMP)

To a 38ml screw capped ace pressure tube were added 3,5-dibromopyridine (0.1g, 0.422 mmol), and trifluoromethoxyphenyl boronic acid (0.104g, 0.506 mmol), K_3PO_4 (0.134g, 0.632 mmol) in distilled water and dioxane (1ml, 3ml), and $\text{Pd}(\text{PPh}_3)_4$ (1.5mol%). After adding all material the ace pressure tube was sealed with screw-cap, placed in the aluminum metal block and heated up to 100 °C for a period of 8 hours. Completion of reaction was confirmed with help of TLC and the reaction mixture were extracted three times with ethyl acetate (3×20 mL), the solvent was evaporated on rotary evaporator at reduced pressure and the crude obtained was re-dissolved in CHCl_3 (5 mL) and contents were taken 250ml round bottom flask and the crude from reaction mixture was adsorbed on silica to make slurry and was loaded on 50 Cm long Silica-Gel column and eluted with n-hexane: ethyl acetate (98: 2 → 97: 3 → 95: 5). The fractions containing the major compound were combined together and evaporated on Rotavap to get major compound as

white amorphous solid. Melting Point = 172-174 °C, Yield 87%; ¹H NMR (500 MHz, Chloroform-d) δ: 8.82 (s, 2H, H-2,6), 7.99(s, 1H, H-4), 7.67-7.65 (d, *J*=2Hz, 4H, H-2',2'',6',6''), 7.37-7.36 (d, *J*=2Hz, 4H, H-3',3'',5',5''); ¹³CNMR (125 MHz, Chloroform-d) δ: 149.49 (C-2,6), 147.28 (C-4), 136.27 (C-1', 1''), 135.53 (C-3,5), 132.86 (C-4), 128.75 (C-2', 2'', C-6', 6''), 121.67 (C-3', 5', 3'', 5''); ¹⁹F NMR (470 MHz, Chloroform-d): δ = -57.80 (s, 6F).

3,5-bis(4-bromophenyl)pyridine (BBPP)

To the 3,5-dibromopyridine (0.1g, 0.422 mmol) and 4-bromophenyl boronic acid (0.19g, 0.97 mmol) in distilled water and dioxane (1ml, 3ml) and K₃PO₄ (0.268g, 1.26 mmol) added Pd(PPh₃)₄ (3.0eq) at 100 °C in dried pressure tube. Product was white amorphous solid. Melting Point = 199-201 °C; Yield 85%; ¹H-NMR (400 MHz, CDCl₃) δ: 8.83-8.82 (d, *J*=1Hz, H-2,6) 8.00-7.98 (t, *J*=1Hz, H-4), 7.68-7.64 (m, *J* = 4Hz, H-2',2'',6',6''), 7.38-7.35 (d, *J*= 3Hz, H-3',3'',5',5''); ¹³C-NMR (75 MHz, CDCl₃) δ: 149.25 (C-2,6), 133.57 (C-4), 134.72 (C-3,5), 135.83 (C-1', 1''), 128.65 (C-2', 2'', C-6', 6''), 122.48 (C-3', 5', 3'', 5''), 124.51 (C-4',4'').

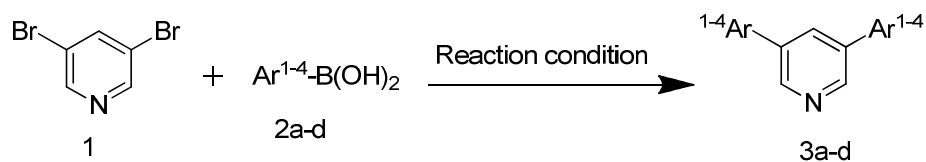
3,5-bis(4-phenoxyphenyl)pyridine (BPPP)

To the 3,5-dibromopyridine (0.1g, 0.422 mmol) and 4-phenoxyphenyl boronic acid (0.198g, 0.928 mmol) in distilled water and dioxane (1ml, 3ml) and K₃PO₄ (0.134g, 0.632 mmol) added Pd(PPh₃)₄ (1.5eq) at 100 °C in dried pressure tube. Product was white crystalline solid. Melting Point = 209-210 °C; Yield 85%; ¹H-NMR (400 MHz, CDCl₃) δ: 8.93 (H-2,6) 7.88 (H-4), 7.75 (H-2', 2'',6',6''), 7.08 (H-3', 3'',5',5''), 7.02 (H-2''', 2''',6''',6'''), 7.37 (H-3''', 3''',5''',5'''), 7.01 (H-4''', 4'''); ¹³C-NMR (75 MHz, CDCl₃) δ: 148.21 (C-2,6), 132.83 (C-4), 133.75 (C-3,5), 130.32 (C-1',1''), 128.74 (C-2',2'',6',6''), 117.91 (C-3', 5', 3'', 5''), 156.25 (C-4',4''), 156.34 (C-1''',1'''), 119.53 (C-2''',2''',6''',6'''), 127.72 (C-3''', 3''',5''',5'''), 121.23 (C-4''',4''').

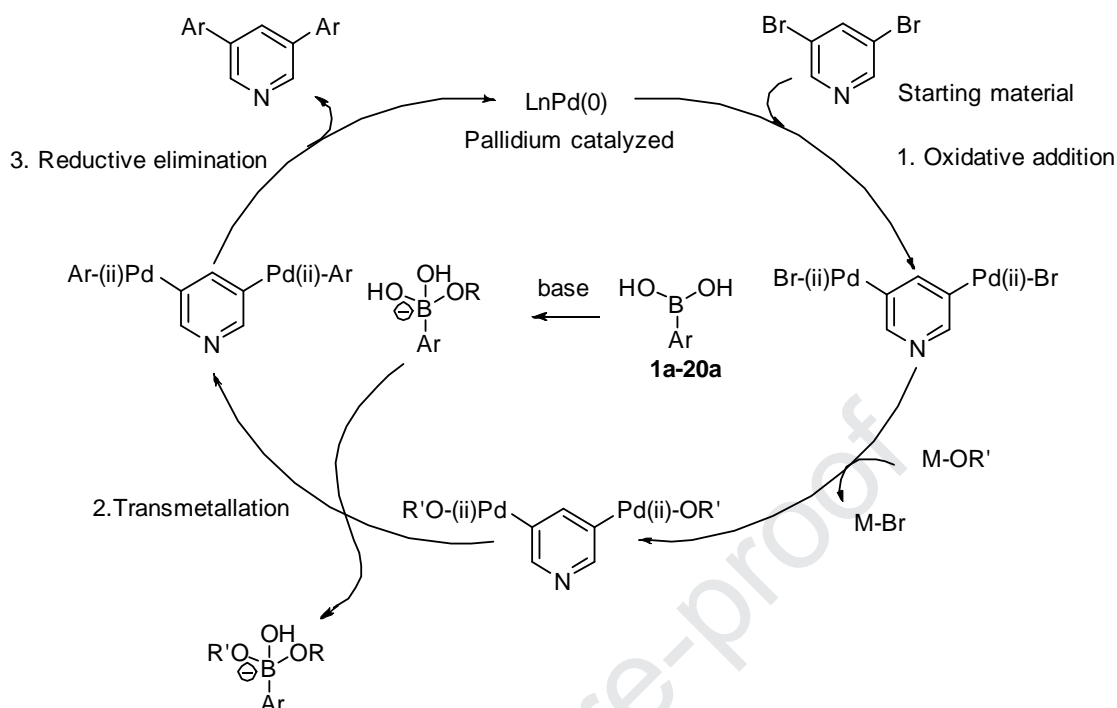
3,5-bis(2,5-dimethoxyphenyl)pyridine(BDMPP)

To the 3,5-dibromopyridine (0.1g, 0.422 mmol) and 2,5-dimethoxyphenyl boronic acid (0.169g, 0.928 mmol) in distilled water and dioxane (1ml, 3ml) and K₃PO₄ (0.134g, 0.632 mmol) added Pd(PPh₃)₄ (1.5eq) at 100 °C in dried pressure tube. Product was white crystalline solid. Melting Point = 226-228 °C; Yield 92%; ¹H-NMR (400 MHz, CDCl₃) δ: 8.91 (H-2,6), 7.86 (H-4), 6.88 (H-2',2'',6',6''), 6.76 (H-4',4''), 3.78 (4×O-Me); ¹³C-NMR (75 MHz, CDCl₃) δ: 148.24 (C-2,6), 132.82 (C-4), 133.71 (C-3,5), 126.93 (C-1',1''), 148.8 (C-2',2''), 112.20 (C-3',3''), 116.21 (C-4',4''), 154.14 (C-5',5''), 111.90 (C-6',6''), 55.8 (4×OMe).

Herein we show plausible mechanism for synthesis of novel arylated pyridines (**BTFMP**, **BBPP**, **BPPP** and **BDMPP**).



Product	Ar ¹⁻⁴ -B(OH) ₂	Yield %
3a-BTFMP		87%
3b-BBPP		85%
3c-BPPP		85%
3d-BDMPP		92%



Scheme 1: Synthesis of derivatives of arylated pyridines.

Computational Procedure

The quantum chemical calculations for four phenyl pyridine derivatives: 3,5-bis(4-(trifluoromethoxy)phenyl)pyridine (**BTfMP**), 3,5-bis(4-bromophenyl)pyridine (**BBPP**), 3,5-bis(4-phenoxyphenyl)pyridine (**BPPP**) and 3,5-bis(2,5-dimethoxyphenyl)pyridine (**BDMPP**), were accomplished with the assistance of DFT using Gaussian 09 program package [20-23]. The SC-XRD driven crystal structures were used as the initial geometry for DFT study. Complete geometrical optimization was done without symmetry restrictions by applying B3LYP level of DFT and 6-311G(d,p) basis set. The DFT/B3LYP/6-311G(d,p) level of theory was used for frequency analysis to obtain additional confirmation of stability related to optimized geometries. NBO analysis was additionally administered at same level of theory and basis set using NBO 3.1 program package [24]. FMOs and NLO analysis was conducted at B3LYP level of DFT with 6-311G(d,p) basis set. The input files were organized with the assistance of Gaussview 5.0. [25] Avogadro [26], Gauss Sum [27] and Chemcraft programs [28] were used for deciphering output files. We used Koopman's theorem [29] to calculate the electronegativity, chemical potential, electrophilicity index and global hardness by using following equations.

Global hardness	$\eta = \frac{I-A}{2}$	Equation 1
Electronegativity	$X = \frac{I+A}{2}$	Equation 2
Global softness	$\sigma = \frac{1}{2\eta}$	Equation 3

We used Parr *et al.* [30-37] concept to obtain the electrophilicity index considered as a reactivity index was calculated by following equation.

Electrophilicity Index	$\omega = \frac{\mu^2}{2\eta}$	Equation 4
------------------------	--------------------------------	------------

η = global hardness, I = ionization energy, A = electron affinity, X = electro negativity, σ = global softness, μ = chemical potential

Results and discussion

The molecules of 3,5-bis(4-phenoxyphenyl)pyridine (**BPPP**) [Figure 1] are symmetric w. r. t. mirror plane passing through N and C-atoms in the pyridine ring. In this molecule, the phenoxy group A (C1-C6/O1), benzene ring B (C7-C12) and pyridine ring (C13-C15/C14ⁱ/C15ⁱ/N1 i = x, -y+1/2, z) are planar with r. m.s. deviation of 0.0299, 0.0020 and 0.0015 Å, respectively. The dihedral angle between A/B, A/C and B/C is 63.87 (5)°, 37.22 (8)° and 32.77 (6)°, respectively [Table 1]. There are no classical H-bonds. There are C-H... π and π ... π interaction which stabilize the molecules. The packing diagram is shown in Figure 2.

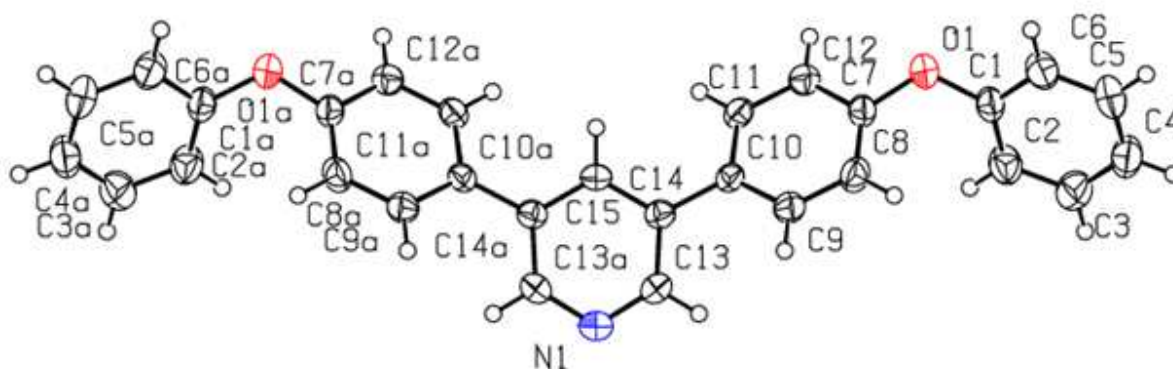


Figure1: ORTEP diagram of 3,5-bis(4-phenoxyphenyl)pyridine (**BPPP**) is drawn with thermal ellipsoids at 50 % probability level with H-atoms as small circles of arbitrary radii. The labeling of symmetry related atoms has been shortened.

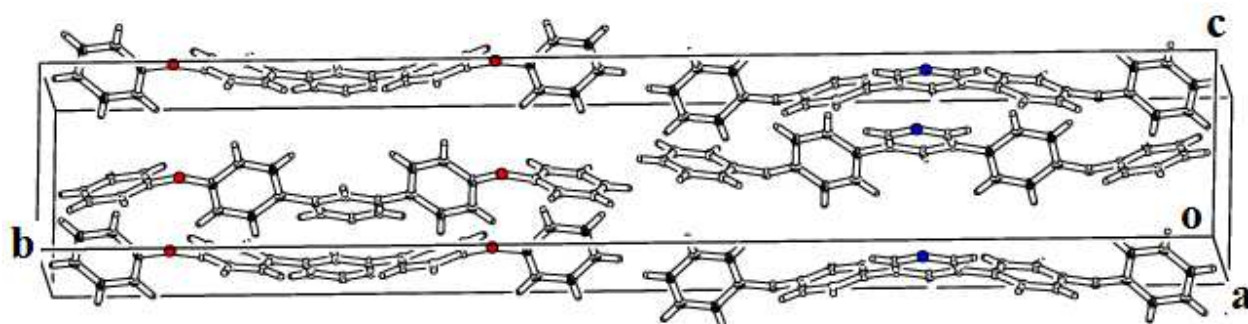


Figure2: The packing diagram of **BPPP**.

In the molecule of 3,5-bis(2,5-dimethoxyphenyl)pyridine (**BDMPP**) [Figure 3], the phenyl groups A (C2-C7) and B (C14-C19) of 2,5-dimethoxyphenyl groups are planar with r. m.s. deviation of 0.0065 and 0.0044 Å, respectively. The pyridine ring C (C9-C13//N1) is also planar with r. m.s. deviation of 0.0033 Å. The dihedral angle between A/B, A/C and B/C is 89.67 (5)°, 53.80 (5)° and 53.70 (5)°, respectively [Table 1]. There are no classical H-bonds in **BDMPP**. There is a C-H...O bonding in **BDMPP** which stabilize the molecules. The weak non classical hydrogen bonding in **BDMPP** is C(21)–H(21)...O(3) with bond distance of 0.96 Å for C(21)–H21, bond length of 2.59 Å for H(21)–O3 is and total distance of 3.325 Å for C21...O3. The bond angle due to $\angle(C(21)–H(21)...O(3))$ is 134°. The H-bonding is shown in Figure 4.

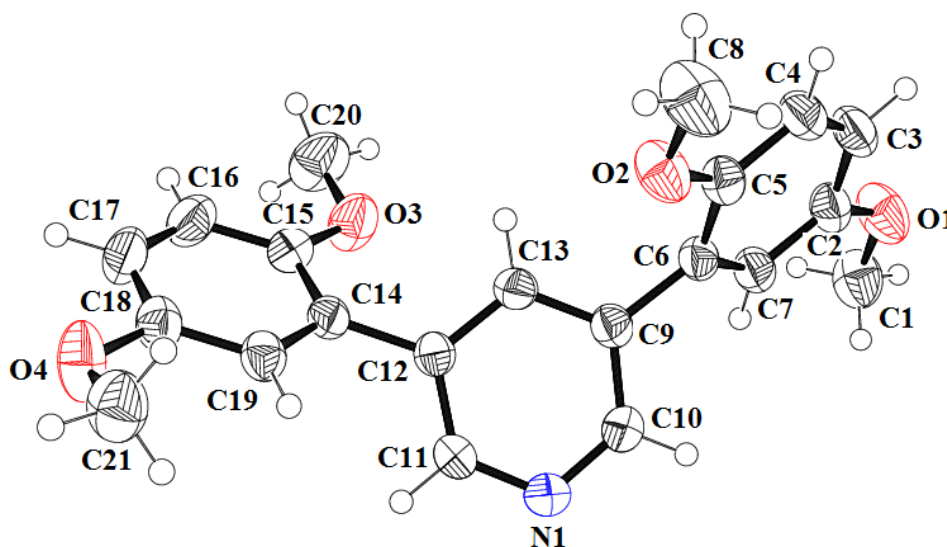


Figure3: ORTEP diagram of 3,5-bis(2,5-dimethoxyphenyl)pyridine (**BDMPP**) is drawn with thermal ellipsoids at 50 % probability level with H-atoms as small circles of arbitrary radii. CIF= ORTEP ; N5= N1, C16= C10, C17= C9, C19= C6, C20=

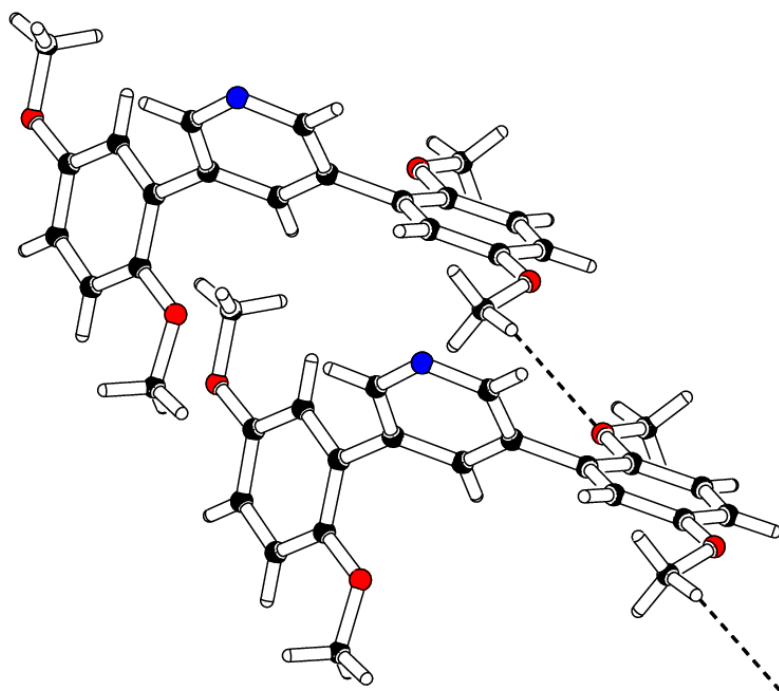


Figure 4: The C-H...O bonding in **BDMPP**.

Table 1: X-ray crystallographic data of **BPPP** and **BDMPP**.

Crystal parameters	BPPP	BDMPP
CCDC #	1947662	1947663
Chemical formula	C ₂₉ H ₂₁ NO ₂	C ₂₁ H ₂₁ NO ₄
<i>M_r</i>	415.47	351.39
Crystal system, space group	Orthorhombic, <i>Pnma</i>	Monoclinic, <i>P2₁/n</i>
Temperature (K)	296	296
<i>a, b, c</i> (Å)	6.4236 (5), 45.035 (3), 7.3855 (5)	13.0552 (11), 8.8528 (7), 16.3557 (14)
β (°)		103.646 (2)
<i>V</i> (Å ³)	2136.5 (3)	1837.0 (3)
<i>Z</i>	4	4
Radiation type	Mo <i>K</i> α	Mo <i>K</i> α
μ (mm ⁻¹)	0.08	0.09
Crystal size (mm)	0.35 × 0.30 × 0.22	0.40 × 0.32 × 0.30
Data collection		

Diffractionmeter	Bruker Kappa APEXII CCD	Bruker Kappa APEXII CCD
Absorption correction	Multi-scan (<i>SADABS</i> ; Bruker, 2005)	Multi-scan (<i>SADABS</i> ; Bruker, 2005)
T_{\min} , T_{\max}	0.973, 0.982	0.966, 0.974
No. of measured, independent and observed [$I > 2\sigma(I)$] reflections	17906, 2367, 1779	15389, 4006, 3040
R_{int}	0.034	0.024
$(\sin \theta/\lambda)_{\text{max}}$ (\AA^{-1})	0.639	0.639
Refinement		
$R[F^2 > 2\sigma(F^2)]$, $wR(F^2)$, S	0.052, 0.131, 1.09	0.041, 0.115, 1.02
No. of reflections	2367	4006
No. of parameters	148	239
H-atom treatment	H-atom parameters constrained	H-atom parameters constrained
$\Delta\rho_{\text{max}}$, $\Delta\rho_{\text{min}}$ (e \AA^{-3})	0.23, -0.20	0.18, -0.16

Computer programs: *APEX2* (Bruker, 2007), *SAINT* (Bruker, 2007), *SHELXS97* (Sheldrick, 2008), *SHELXL2014/6* (Sheldrick, 2015), *ORTEP-3 for Windows* (Farrugia, 1997) and *PLATON* (Spek, 2009), *WinGX* (Farrugia, 1999) and *PLATON* (Spek, 2009).

Molecular geometric parameters

As we have discussed already the compounds (**BPPP**) and (**BDMPP**) exist in the form of crystals among studied compounds. Therefore, SC-XRD has been performed just for **BPPP** and **BDMPP**. Herein, we will compare SC-XRD based parameters of **BPPP** and **BDMPP** with DFT based structural parameters. The obtained parameters were tabulated in Table S1 and S2 (Supplementary Information) for **BPPP** and **BDMPP** respectively. The comparative study was done between DFT computed and experimentally determined parameters.

The exact same DFT and XRD determined values of bond lengths in **BPPP** has been found to be 1.333 Å for both N1-C13a and N1-C13 while that for **BDMPP** was found to be 1.37 Å for O2-C5. While the minimum deviation between DFT and XRD determined values of bond lengths in **BPPP** has been found to be 0.001 Å for O1a-C1a, C10a-C14a, O1-C1 and C10-C14. In the same way, the minimum deviation of 0.001 Å was found in **BDMPP** for O4-C18. Moreover, the maximum deviation between DFT and XRD determined values of bond lengths in **BPPP** has been found to be 0.025 Å for C4a-C5a and C4-C5 and 0.024 Å for C3a-C4a and C3-C4. While that of **BDMPP** were found to be 0.018 Å for C12-C11, 0.017 Å for C18-C17 and 0.016 Å for C10-C9.

The exact same DFT and XRD determined values of bond angles in **BPPP** has been found to be 120.8° , 119.6° and 121.6° for C1a-O1a-C7a, C3a-C4a-C5a and C8a-C9a-C10a respectively while that for **BDMPP** was found to be 119.2° and 119.7° for C19-C18-C17 and C6-C5-C4 respectively. The minimum deviation between DFT and XRD determined values of bond angles in **BPPP** has been found to be 0.1° for O1a-C1a-C2a, C2a-C1a-C6a and C2a-C3a-C4a. Similarly, in **BDMPP** has found to be 0.1° for C21-O4-C18, C15-O3-C20 and C11-C12-C13. Moreover, the maximum deviation between DFT and XRD determined values of bond angles in **BPPP** has been found to be 1.7° for C13a-N1-C13 while that of **BDMPP** was found to be 1° for C11-N1-C10, C15-C14-C12 and C14-C12-C11.

Overall, bond lengths and bond angles in both derivatives are deviated in the ambient range of $0.025\text{-}0.0\text{\AA}$ and $0.0\text{-}1.7^\circ$ respectively. The comparative analysis revealed that DFT values of bond angles and bond lengths were higher than XRD values. However, in a few cases the opposite happened as the DFT values of bond angles and bond lengths were smaller than the XRD values. The dissimilarity between DFT and experimental findings could be because of the medium effect[38].

FT-IR Analysis

DFT studies were conducted to have a clear understanding of vibration modes of entitled compounds in solvent free conditions. The animation option available in Avogadro software was used for assigning vibration modes related to the specific structural features of entitled compounds. The quantity of atoms in **BTFMP**, **BBPP**, **BPPP** and **BDMPP** are 39, 31, 53 and 47 atoms respectively with symmetry point group C1. Their experimental spectra can be seen in Figures S1-S4.

C-H stretching vibration

In **BTFMP**, the aromatic ring carbon-hydrogen (C-H) stretching frequencies are found in the range of $3206\text{-}3153\text{ cm}^{-1}$ (DFT) and 2922 cm^{-1} (EXP) (Figure S1). For **BBPP**, carbon-hydrogen (C-H) stretching frequencies of the aromatic ring are located in the span of $3204\text{-}3152\text{ cm}^{-1}$. In **BPPP**, the aromatic ring (C-H) stretching frequencies are appeared at $3199\text{-}3151\text{ cm}^{-1}$ range (DFT) and $3066\text{-}2922\text{ cm}^{-1}$ (EXP) in Figure S2. Further, in **BDMPP**, the aromatic ring (C-H) stretching modes are occurred at $3225\text{-}3000\text{ cm}^{-1}$ range (DFT) and $2951.09\text{-}2900\text{ cm}^{-1}$ range (EXP) in Figure S3.

C-C stretching vibrations

The C-C stretching vibrations are appeared in the range of 1645-1538, 1628-1339, 1649-1518 and 1643-1535 cm^{-1} for **BTFMP**, **BBPP**, **BPPP** and **BDMPP** respectively which are found in correspondence to experimental values: 1509-1499 cm^{-1} (Figures S1-S4)

C-N stretching vibrations

The C-N stretching modes are observed at 3206, 1618, 1038 and 664 cm^{-1} in **BTFMP**. Similar modes are observed at 1626, 1304 and 653 cm^{-1} in **BBPP**. Likewise, FTIR bands are found at 1625, 1259 and 634 cm^{-1} in **BPPP**. The C-N modes of **BDMPP** are appeared at 1628, 1264, 1044 and 660 cm^{-1} . The experimental modes are found as 1506.45 for **BTFMP** and 1585.49 cm^{-1} for **BBPP** and **BDMPP** in Figures S1-S4.

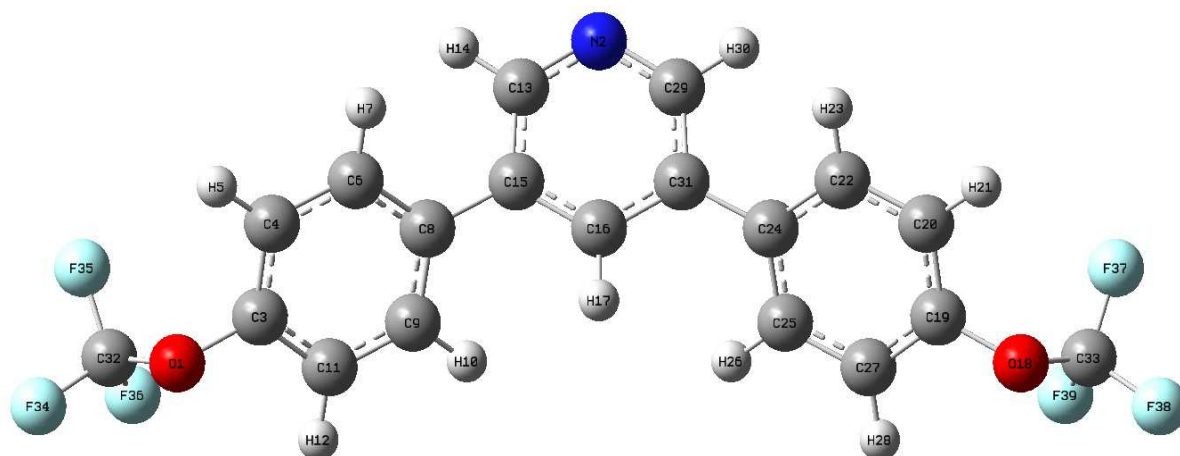
Natural Bond Orbital (NBO) Analysis

Inspection of inter and intramolecular interactions can be adequately accomplished using natural bond orbital (NBO)[39] analysis, which contributes promising facts for exploring charge transfer or hyper-conjugative synergy. The software named NBO 3.1 is utilized to perform hybridization, intramolecular charge delocalization, and electron density in molecules simulated by Gaussian 09 package. NBO approach can be used to analyses bonding and anti-bonding interactions due to second-order perturbation theory [40]. Second-order stabilization energies $E^{(2)}$ have been acquired using equation 5:

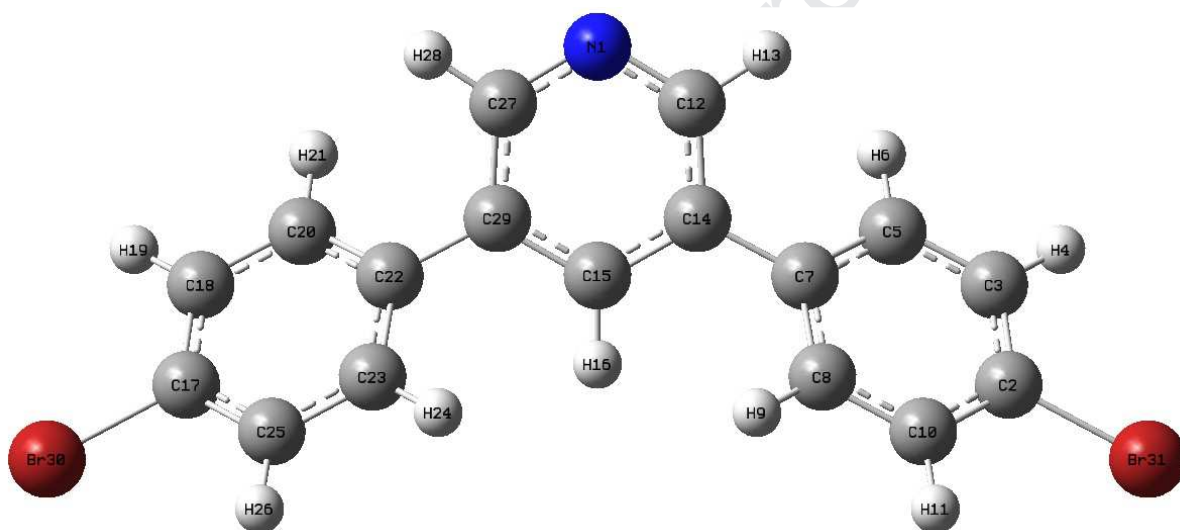
$$E^{(2)} = q_i \frac{(F_{ij})^2}{\epsilon_j - \epsilon_i} \quad \text{Equation 5}$$

Where q_i is the i th donor orbital occupancy, E_j , E_i the diagonal elements (orbital energies) and (j, i) the off diagonal NBO Fock Matrix elements [41].

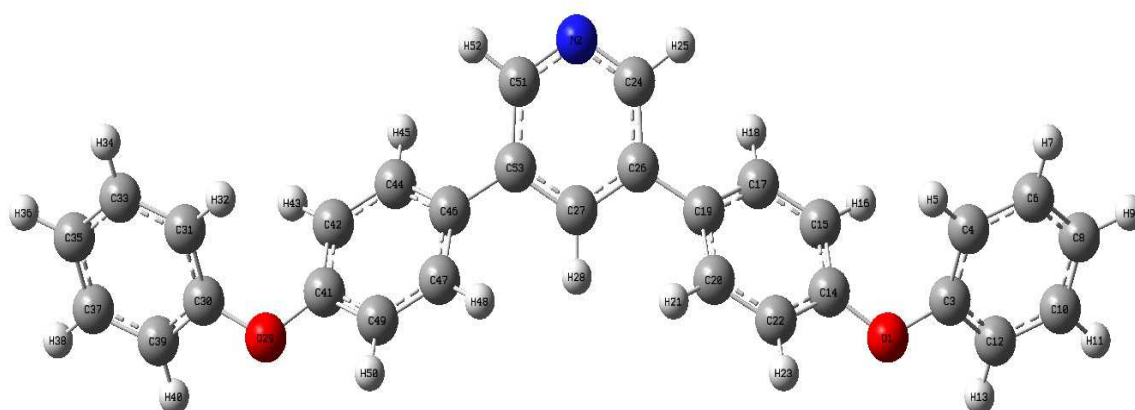
The natural bond orbital (NBO) analysis has been completed for four compounds, i.e., **BTFMP**, **BBPP**, **BPPP** and **BDFMP**. The natural bond orbital (NBO) analyses for **BTFMP**, **BBPP**, **BPPP** and **BDFMP** have been elaborated in Tables S3-S6. While some selected values are given Table 2. The NBO numbering scheme for title compounds are represented in Figure 5.



BTMFP



BBPP



BPPP

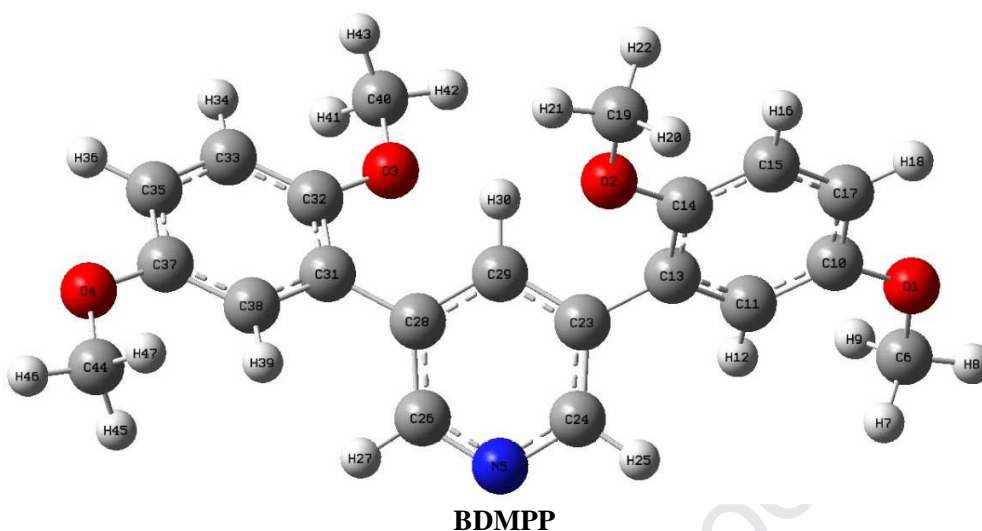


Figure 5: NBO numbering scheme of entitled derivatives

Table 2: Natural bond orbital (NBO) analysis for **BTfMP**, **BBPP**, **BPPP** and **BDMPP** (Representative Values)

Derivative	Donor(i)	Type	Acceptor (j)	Type	$E(2)^a$	$E(j)-E(i)^b$ [a.u.]	$F(i; j)^c$ [a.u.]
BTfMP	C15 - C16	π	N2 - C13	π^*	26.58	0.27	0.076
	N2 - C13	π	C29 - C31	π^*	25.43	0.32	0.082
	C29 - C31	π	N2 - C13	π^*	18.46	0.27	0.063
	N2 - C13	σ	C15 - C16	σ^*	14.19	0.32	0.061
	O1	LP2	C32 - F36	π^*	14.88	0.57	0.083
	O18	LP2	C33 - F39	π^*	14.88	0.57	0.082
	F35	LP2	C32 - F36	σ^*	7.14	0.66	0.062
BBPP	C14-C15	π	N1-C12	π^*	26.56	0.27	0.075
	N1-C12	π	C27-C29	σ^*	25.28	0.32	0.082
	C5-C7	π	C14 -C15	π^*	9.28	0.28	0.046
	C20-C22	π	C27-C29	π^*	9.01	0.28	0.045
	N1	LP	C12-C14	σ^*	10.10	0.88	0.085
	N1	LP	C27-C29	σ^*	10.10	0.88	0.085
	Br30	LP	C17-C18	σ^*	3.41	0.86	0.048
	Br30	LP	C17-C25	σ^*	3.41	0.85	0.048
	Br31	LP	C2-C3	σ^*	3.41	0.86	0.048
Br31	LP	C2-C10	σ^*	3.41	0.85	0.048	
BPPP	C27 - C53	π	N2 - C51	π^*	27.21	0.25	0.074
	C4 - C6	π	C3 - C12	π^*	22.04	0.28	0.071
	N2 - C51	σ	C47 - C49	σ^*	7.10	4.89	0.166
	N2 - C51	σ	C51 - H52	σ^*	6.37	4.98	0.159
	O1	LP2	C14 - C15	π^*	18.77	0.35	0.077
	N2	LP1	C51 - C53	σ^*	9.38	0.89	0.082
BDMPP	C44 - H47	σ	C44 - H45	σ^*	2651.48	0.31	0.807
	C44 - H47	σ	C15 - C17	σ^*	2363.37	0.09	0.406
	O4 - C37	σ	C15 - C17	σ^*	19.86	0.76	0.110
	C13 - C14	π	C10 - C11	π^*	19.33	0.28	0.066
	O2	LP2	C40 - H41	σ^*	519.47	0.01	0.067

O1	LP1	C23 - C29	π^*	10.06	0.34	0.056
----	-----	-----------	---------	-------	------	-------

^aE⁽²⁾ means energy of hyper conjugative interaction (stabilization energy in kcal/mol), ^bEnergy difference between donor and acceptor i and j NBO orbitals, ^cF(i;j) is the Fock matrix element between i and j NBO orbitals.

Tables S3-S6 contain NBO orbitals which show mostly efficient interactions between Lewis type π -(bonding) and non-Lewis (anti-bonding) for the **BTFMP**, **BBPP**, **BPPP** and **BDMPP**. The enhanced stabilization energy E⁽²⁾ values are obtained due to the existence of strong interactions between donor and acceptor moieties.

Herein, NBO analysis revealed that the $\pi(\text{C15-C16}) \rightarrow \pi^*(\text{N2-C13})$ and $\pi(\text{N2-C13}) \rightarrow \pi^*(\text{C29-C31})$ transitions provide strongest stabilization energy values as 26.58 and 25.43 kcal/mol respectively to the compound (**BTFMP**). Further, the stabilization energy values found to be 18.46 and 14.19 kcal/mol for transitions as $\pi(\text{C29-C31}) \rightarrow \pi^*(\text{N2-C13})$ and $\sigma(\text{N2-C13}) \rightarrow \sigma^*(\text{C15-C16})$. The transitions ($\sigma \rightarrow \sigma^*$) originated due to weak interactions which offer small stabilization energy values to the **BTFMP** as can be seen in Table 2. The similar trend of interaction was also observed in reference to resonance in the **BTFMP** as $\text{LP2}(\text{O1}) \rightarrow \pi^*(\text{C32-F36})$ and $\text{LP2}(\text{O18}) \rightarrow \pi^*(\text{C33-F39})$ produced 14.88 kcal/mol each respectively with peak values. While $\text{LP2}(\text{F35}) \rightarrow \sigma^*(\text{C32-F36})$ produced 7.14 kcal/mol which is least value for **BTFMP**.

For **BBPP**, the stabilization energies also obtained to be 26.56 and 25.28 kcal/mol owing to $\pi(\text{C14-C15}) \rightarrow \pi^*(\text{N1-C12})$ and $\pi(\text{N1-C12}) \rightarrow \sigma^*(\text{C27-C29})$ transitions respectively (Table 2). NBO analysis revealed that the $\pi(\text{C5-C7}) \rightarrow \pi^*(\text{C14-C15})$ and $\pi(\text{C20-C22}) \rightarrow \pi^*(\text{C27-C29})$ transitions also give stabilization to the **BBPP** with energy values 9.28 and 9.01 kcal/mol respectively. The identical trend of interaction was also noticed in relation to resonance in the **BBPP** as both $\text{LP}(\text{N1}) \rightarrow \sigma^*(\text{C12-C14})$ and $\text{LP}(\text{N1}) \rightarrow \sigma^*(\text{C27-C29})$ produced 10.10 kcal/mol which was the highest value. While all transitions: $\text{LP}(\text{Br30}) \rightarrow \sigma^*(\text{C17-C18})$, $\text{LP}(\text{Br30}) \rightarrow \sigma^*(\text{C17-C25})$, $\text{LP}(\text{Br31}) \rightarrow \sigma^*(\text{C2-C3})$ and $\text{LP}(\text{Br31}) \rightarrow \sigma^*(\text{C2-C10})$ produced same 3.41 kcal/mol interaction energy. For **BPPP**, the stabilization energy values obtained to be 27.21 and 22.04 kcal/mol for transitions as $\pi(\text{C27-C53}) \rightarrow \pi^*(\text{N2-C51})$ and $\pi(\text{C4-C6}) \rightarrow \pi^*(\text{C3-C12})$ respectively (Table 2). While transitions as $\sigma(\text{N2-C51}) \rightarrow \sigma^*(\text{C47-C49})$ and $\sigma(\text{N2-C51}) \rightarrow \sigma^*(\text{C51-H52})$ exposed 7.10 and 6.37 kcal/mol respectively. These transitions originated due to weak interactions between the donor π/σ and acceptor π^*/σ^* and offer small stabilization to **BPPP** (Table 2). The same tendency of interaction was also noted regarding to resonance in

BPPP as $LP2(O1) \rightarrow \pi^*(C14-C15)$ and $LP1(N2) \rightarrow \sigma^*(C51-C53)$ produced 18.77 and 9.38 kcal/mol respectively which are highest values.

The highest interactions in **BDMPP** have $\sigma(C44-H47) \rightarrow \sigma^*(C44-H45)$ and $\sigma(C44-H47) \rightarrow \sigma^*(C15-C17)$ leads to the stabilization energy of 2651.48 and 2363.37 kcal/mol respectively (Table 2). These values were found the enormous values among all the stabilization energies. Moreover, other representative interactions are observed as $\sigma(O4-C37) \rightarrow \sigma^*(C15-C17)$ and $\pi(C13-C14) \rightarrow \pi^*(C10-C11)$ with stabilization energy values like 19.86 and 19.33 kcal/mol respectively. The $LP2(O2) \rightarrow \sigma^*(C40-H41)$ transition shows the stabilization energy of 519.47 kcal/mol which was the highest value. While $LP1(O1) \rightarrow \pi^*(C23-C29)$ shows 10.06 kcal/mol which was exhibited a very low interaction energy (Table 2). A bunch of stabilization energy values were shown in Tables S3-S6 despite of representative NBO values of **BTFMP**, **BBPP**, **BPPP** and **BDMPP**. It might be deduced from NBO results that the strong intra-molecular hyper conjugation interactions are the crucial for the stability of these compounds.

Natural Population Analysis (NPA)

The Mulliken atomic charges of the **BTFMP**, **BBPP**, **BPPP** and **BDMPP** were determined and presented in Figure 6. The phenomenon associating the electronegativity equalization can be explained through Mulliken population examination and atomic charge transformation process takes place in reactions and to obtain the electrostatic potential on external surfaces of systems [42]. The electronic charges of atoms play a significant function for molecular conformation as well as bonding capability [43]. The data of Mulliken population disclose that more electronegative atoms as O and N in title compounds make unequal redistribution of the electron density over the benzene rings [44]. Our concern is to illustrate the electron distribution over the title compounds and also to explore their reactive sites. Moreover, Mulliken population analysis displays that no discrepancy is observed regarding charge distribution over all the hydrogen atoms. The positive charges over the hydrogen atoms are found as a result of the negative charges of carbon atoms. The fluoro and bromo atoms are presented in **BTFMP** and **BBPP** contain high negative charges. Mostly carbon, all oxygen and nitrogen atoms with negative charges are found in **BTFMP**, **BBPP**, **BPPP** and **BDMPP** (see Figure 6).

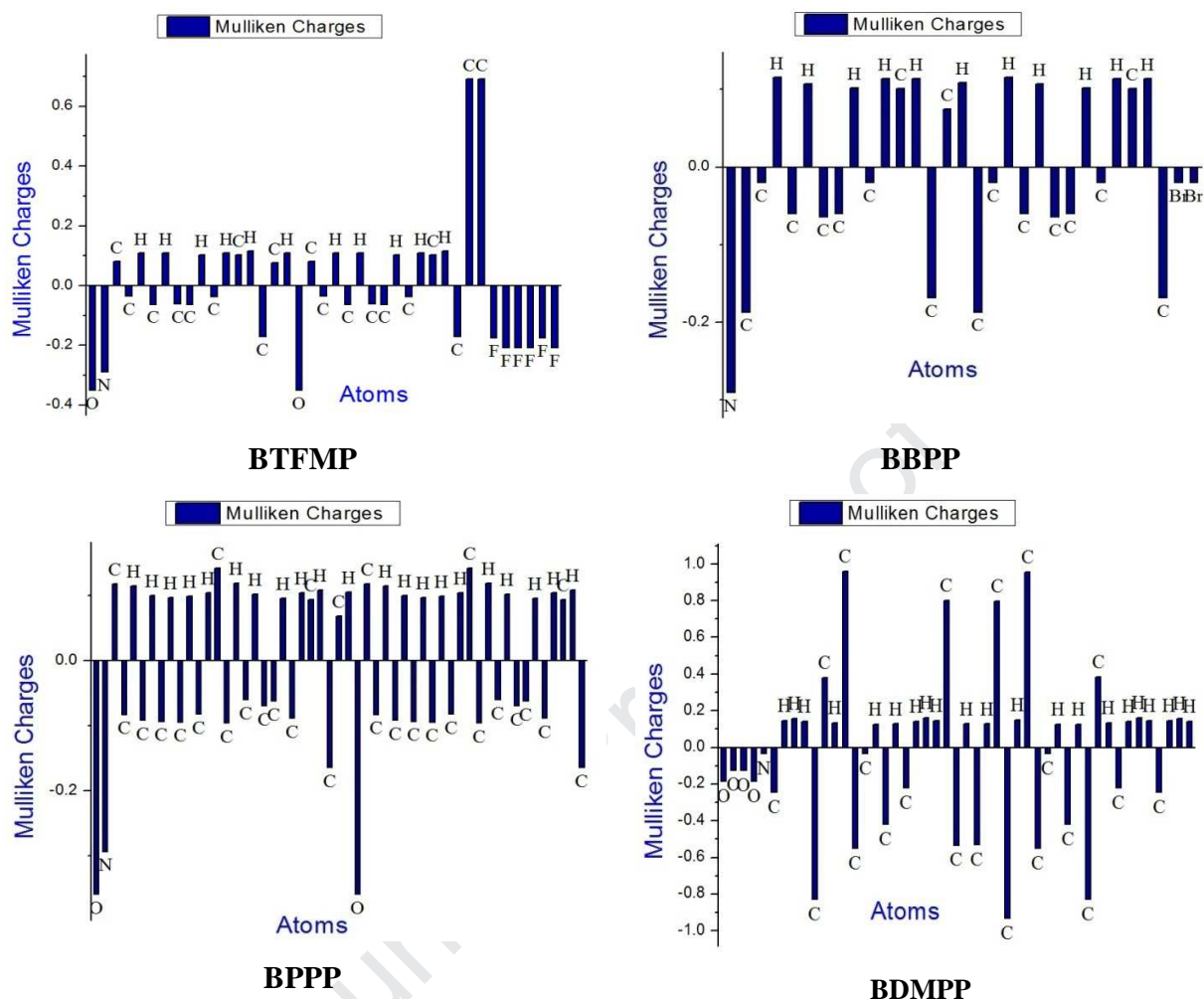


Figure 6. Natural population analysis of entitled derivatives

Frontier molecular orbitals (FMOs)

The highest occupied molecular orbital (HOMO) and lowest unoccupied molecular orbital (LUMO) are collectively known frontier molecular orbitals (FMOs) which are valuable descriptors for predicting kinetic stability and chemical reactivity of the chemical system[45]. The energy values of HOMO/LUMO are calculated to be -6.454/-2.230, -6.302/-0.910, -6.017/-1.235 and -5.650/-1.132 eV for **BTFMP**, **BBPP**, **BPPP** and **BDMPP** respectively (Table 3). These molecular orbitals are formed because of the combination of atomic π -electron orbitals. Thus, π -electrons can be readily distorted, that's why the nonlinear optical responsibility is held by FMOs of the investigated compounds. The HOMO and LUMO plots of all derivatives are displayed in Figure 7.

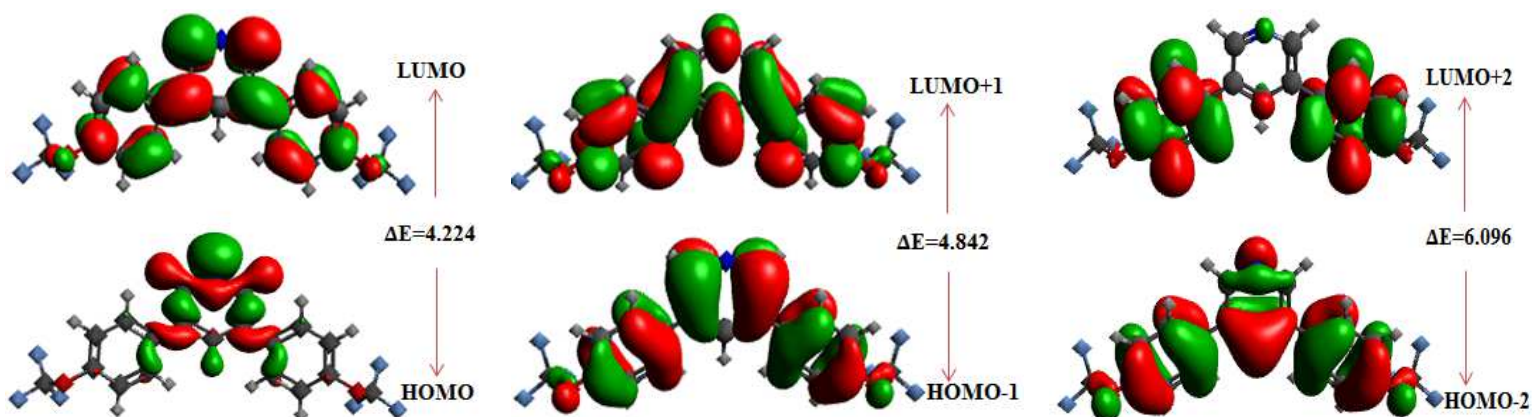
For **BTFMP**, in HOMO, the charge density is accumulated on the 3,5-dimethylpyridine; while, in reference to LUMO, the charge density moves to the (trifluoromethoxy) benzene too. For **BBPP** in case of both HOMO and LUMO the charge density is mainly accumulated on the whole structure of **BBPP**. For **BPPP**, in case of HOMO, the charge density is mainly accumulated on the 3,5-bis(4-phenoxyphenyl)pyridine (**BPPP**), whereas, in case of LUMO, the charge density moves to the 3,5-bis(4-phenoxyphenyl)pyridine (**BPPP**) with the exception of both attached side phenoxy groups. For **BDMPP**, in case of HOMO, the charge density is mainly accumulated on the 3,5-bis(2,5-dimethoxyphenyl)pyridine (**BDMPP**), whereas, in case of LUMO, the charge density moves to the 3,5-diphenylpyridine.

The HOMO-LUMO energy gaps 4.224, 4.290, 4.782 and 4.518eV (Table 2) for **BTFMP**, **BBPP**, **BPPP** and **BDMPP** respectively is comparatively small, which points out that the kinetic stability is fragile but the chemical reactivity of the molecule is forcible in terms of strengthens. Density of States (DOS) of the **BTFMP**, **BBPP**, **BPPP** and **BDMPP** was determined using the GaussSum software which is shown in Figure 7.

Table 3: Frontier Molecular Orbitals Energy calculated for **BTFMP**, **BBPP**, **BPPP** and **BDMPP**.

Articles	BTFMP		BBPP		BPPP		BDMPP	
MO(s)	Energy (eV)	ΔE (eV)	Energy (eV)	ΔE (eV)	Energy (eV)	ΔE (eV)	Energy (eV)	ΔE (eV)
HOMO	-6.454	4.224	-6.302	4.290	-6.017	4.782	-5.650	4.518
LUMO	-2.230		-0.910		-1.235		-1.132	
HOMO-1	-6.595	4.842	-6.662	4.672	-6.194	5.006	-5.701	4.679
LUMO+1	-1.753		-1.990		-1.188		-1.022	
HOMO-2	-7.128	6.096	-7.427	6.517	-6.836	6.089	-6.621	6.317
LUMO+2	-1.032		-2.012		-0.747		-0.304	

HOMO = Highest Occupied Molecular Orbital, LUMO = Lowest Unoccupied Molecular Orbital



BTFMP

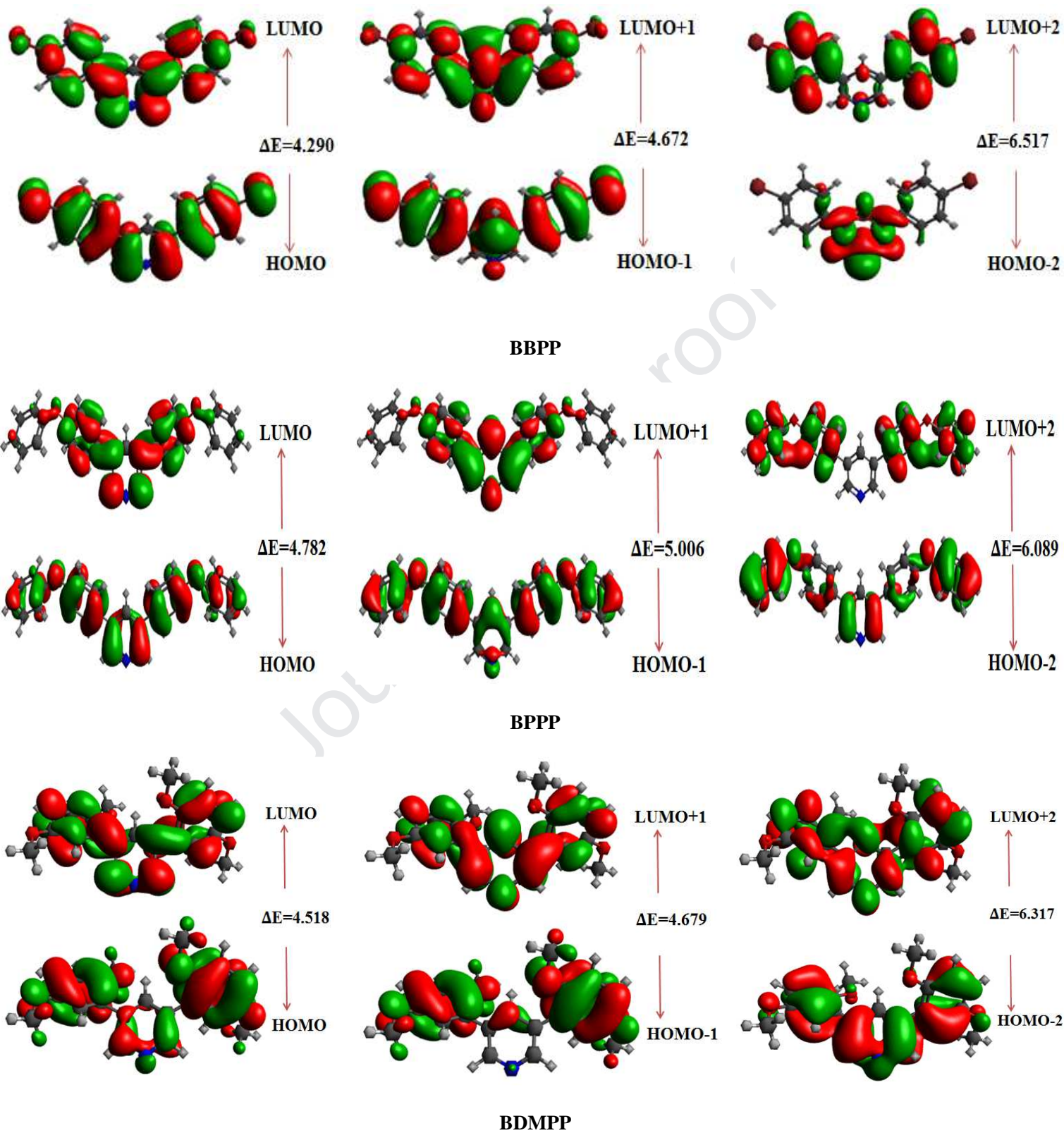


Figure 7: Two levels below & up of HOMO & LUMO orbitals of entitled derivatives and units in eV.

Global Reactivity Parameters

Energies of HOMO, LUMO and their energy gaps are therefore employed to indicate the stability and reactivity of **BTFMP**, **BBPP**, **BPPP** and **BDMPP** by predicting global reactivity descriptors. The popular Koopmans' theorem [29] explains electron affinity (EA) and ionization potential (IP) by the negative of energy eigen values of LUMO and HOMO respectively.

$$EA = -E_{LUMO} \quad \text{Equation 6}$$

$$IP = -E_{HOMO} \quad \text{Equation 7}$$

Equations 6 and 7 defined as EA= Electron affinity, IP= Ionization potential;

Those compounds are known electron acceptors which contain positive electron affinity values and could be participated in charge transfer processes. In our investigation, **BTFMP**, **BBPP**, **BPPP** and **BDMPP** also consisting of positive electron affinity values as 2.23, 0.91, 1.235 and 1.132 eV respectively. Therefore, it is also known electron acceptors by nature and may be involved to charge transfer processes. Whereas, **BTFMP**, **BBPP**, **BPPP** and **BDMPP** contain highly positive ionization potential values as 6.454, 6.302, 6.017 and 5.65 respectively. These high values of IP point out the high reactivity of entitled molecules. IP and EA are frequently utilized as electronic descriptors; also have the positive point that they are conveniently accessible from theory point of view and experimental aspects. IP is a scale for degree of the nucleophilicity of a compound. EA is a scale for degree of the effectiveness of the chemical system to afford the corresponding negative ion.

The reactivity assessment of compound is one of the most significant aims of computational analysis and many reports are available related to this topic in the literature. DFT is one of the most successful theories in contributing theoretical accomplishments of trustworthy qualitative chemical ideas [30]. In current study, various reactivity descriptors are predicted which are utilized to study the site selectivity as well as chemical reactivity. The global softness, electronegativity, global hardness, electrophilicity index and chemical potential are frequently adopted global reactivity parameters which are used to comprehend the global nature of chemical species in reference to their reactivity and stability.

Table 4: The calculated global reactivity parameters of studied compounds.

Compounds	I	A	X	η	μ	ω	σ
-----------	---	---	---	--------	-------	----------	----------

BTFMP	6.454	2.23	4.342	2.112	-4.342	4.463	0.237
BBPP	6.302	0.91	3.606	2.696	-3.606	2.412	0.186
BPPP	6.017	1.235	3.626	2.391	-3.626	2.750	0.209
BDMPP	5.65	1.132	3.391	2.259	-3.391	2.545	0.221

Ionization potential (I), electron affinity (A), electronegativity (X), global hardness (η), chemical potential (μ), global electrophilicity (ω) and global softness (σ).

The calculated results of **BTFMP**, **BBPP**, **BPPP** and **BDMPP** are shown in Table 4. The electronegativity illustrates the tendency of attraction of electron might in the direction of functional moiety, which is known a chemical property. The entitled molecules: **BTFMP**, **BBPP**, **BPPP** and **BDMPP** contain 4.342, 3.606, 3.626 and 3.391 eV electronegativity values respectively (Table 4). The **BTFMP** contains high electronegativity value as compared to other derivatives due to the presence of fluoro group. The **BTFMP**, **BBPP**, **BPPP** and **BDMPP** contain the negative values to the chemical potential (μ) like -4.342, -3.606, -3.626 and -3.391 eV respectively (Table 4). These values explain that the all derivatives are favorably stable and such molecules could not be decomposed by spontaneous way into their fundamental elements. However, the compounds contain positive chemical potential are really unstable and are found challenging to synthesize as well as conserve.

Chemical hardness figures out the shield the alteration for the electronic distribution framework as in a collection of electrons and nuclei. The chemical compound with a large HOMO-LUMO energy difference is assimilated as hard chemical specie, contrarily, the chemical compound with having a small HOMO-LUMO energy gap is assimilated as chemical specie. The soft chemical species have more capacity to polarize in the comparison of the hard ones because the excitation of such molecules requires less amount of energy.

The global hardness values are observed as 2.112, 2.696, 2.391 and 2.259 eV for **BTFMP**, **BBPP**, **BPPP** and **BDMPP** respectively, contrary, the softness values are observed as 0.237, 0.186, 0.209 and 0.221 eV for **BTFMP**, **BBPP**, **BPPP** and **BDMPP** respectively (Table 4). These values highlighted that the title molecules are relatively hard so they do not tend to go through in to reactions or changes conveniently.

The global electrophilicity index defines the stabilization energy when the compound obtains an

extra charge from the surroundings. It indicates the stabilization energy of the compounds when they become full with electrons arriving from the environment. In the entitled molecules they are calculated to be 4.463, 2.412, 2.750 and 2.545 eV for **BTFMP**, **BBPP**, **BPPP** and **BDMPP** respectively (Table 4). The electrophilicity values contain insights regarding reactivity, structural and selectivity factors of ground and excited electronic states of molecules.

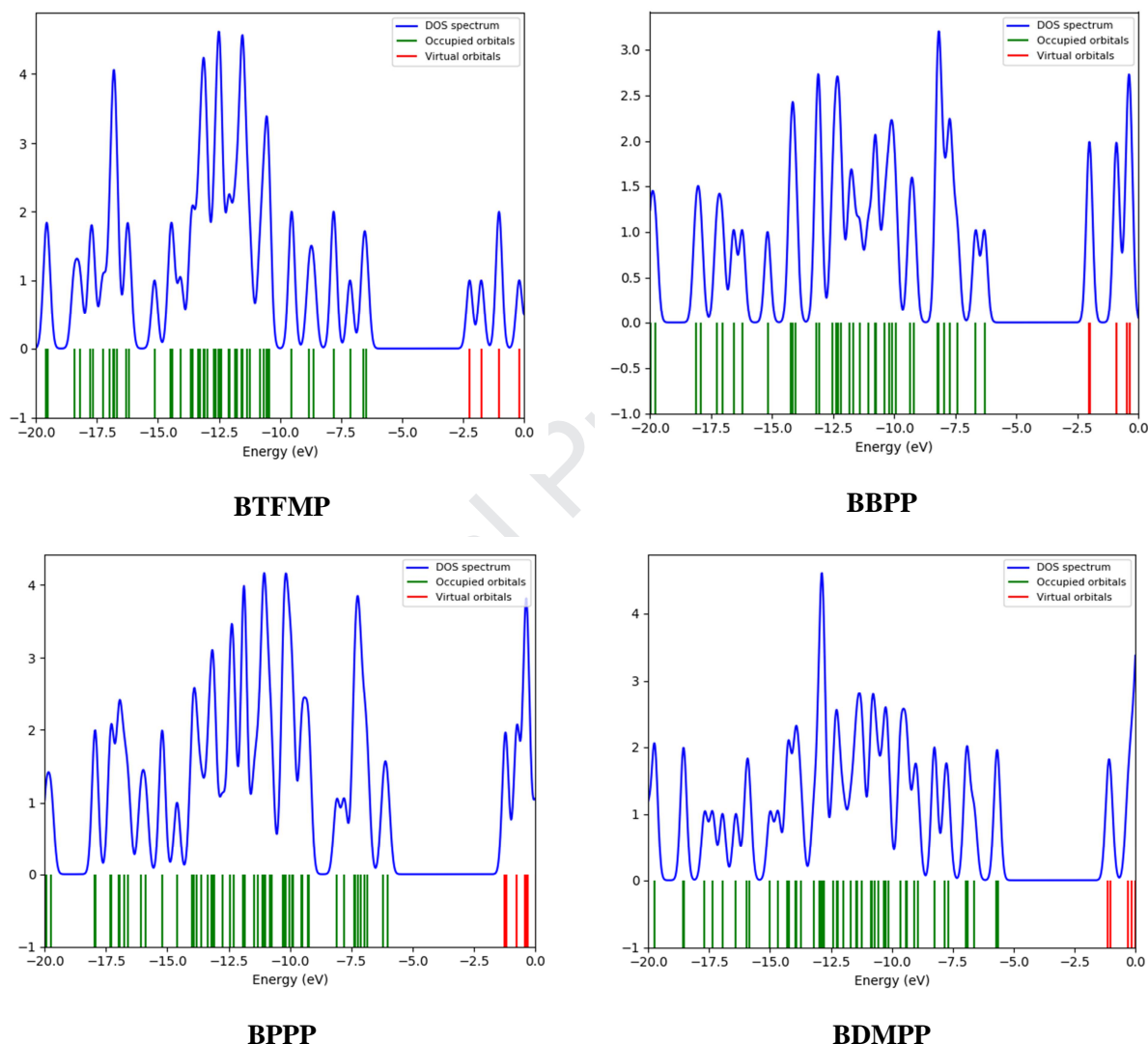


Figure 8: Density of states for entitled derivatives.

Non-Linear Optical (NLO) Properties

In recent years, chemist community is performing extensive investigation and successive improvement in the nonlinear optics (NLO) field[46-47]. Inorganic and organic materials due to their significance in giving the key role of frequency shifting, optical switching, optical modulation, optical memory and optical logic for the modern sophisticated technologies in fields

like telecommunications, optical interconnections and signal processing[48-52]. Many classes of inorganic and organic NLO compounds were analyzed for their promising electro-optical (EO) functions. Among these classes, organic compounds are considered as effective electro-optical (EO) materials due to their particular and unique structural parameters, which normally consisting of the donor- π , π -acceptor and donor- π -acceptor (D- π -A) configurations[53]. The basic concept of utilizing electron-acceptor and electron-donor groups is to polarize the π -electronic organic compounds. This fundamental concept may become the solid reason for growing the NLO chromophores containing greater improved solubility, molecular nonlinearity, processability and good thermal stability. From the aspect of promising applications to optical devices, we calculated the linear response (polarizability, α) and nonlinear responses (hyperpolarizabilities, β) of **BTFMP**, **BBPP**, **BPPP** and **BDMPP**. The $\langle\alpha\rangle$ values were calculated and results were tabulated in Table 5.

Table 5: Dipole polarizabilities with major contributing tensors (a.u.) and dipole moments of the studied compounds

Polarizability				
	BTFMP	BBPP	BPPP	BDMPP
α_{xx}	356.805	392.940	597.894	365.463
α_{yy}	214.377	216.854	283.147	232.736
α_{zz}	119.755	118.144	197.499	202.300
$\langle\alpha\rangle$	230.312	242.646	359.513	266.833
Dipole moments				
	BTFMP	BBPP	BPPP	BDMPP
<i>X</i>	0.0001	0.0000	0.0000	-0.0011
<i>Y</i>	-0.1464	-0.5796	-0.5320	-2.6456
<i>Z</i>	-0.9299	-0.1262	0.3268	0.1043
<i>total</i>	0.9413	0.5931	0.6244	2.6477

BTFMP, **BBPP**, **BPPP** and **BDMPP** are polar molecules comprising non-zero dipole moments as 0.9413, 0.5931, 0.6244 and 2.6477 respectively. The average polarizability $\langle\alpha\rangle$ of **BTFMP**, **BBPP**, **BPPP** and **BDMPP** contain values 230.312, 242.646, 359.513 and 266.833 respectively. Among studied molecules, **BPPP** contains maximum average polarizability, whereas, **BTFMP** consisting of minimum average polarizability as can be seen in Table 5.

Table 6: The computed second-order polarizabilities (β_{tot}) and major contributing tensors (a.u) of the studied compounds

Polarizability				
	BTFMP	BBPP	BPPP	BDMPP
β_{xxx}	0.018	-0.001	-0.004	-0.301

β_{xxy}	149.230	420.404	1003.489	-21.691
β_{xyy}	0.007	-0.000	-0.000	1.715
β_{yyy}	1.416	97.824	4.540	30.101
β_{xxz}	-28.922	27.117	-123.430	-0.985
β_{yyz}	-9.882	23.335	17.347	-0.543
β_{xzz}	0.003	-0.000	0.000	-1.704
β_{yzz}	21.273	8.660	-25.946	22.844
β_{zzz}	19.462	0.002	-0.040	2.873
β_{total}	173.004	529.298	987.800	31.284

The computed second-order polarizabilities (β_{tot}) of **BTFMP**, **BBPP**, **BPPP** and **BDMPP** contain values 173.004, 529.298, 987.800 and 31.284 respectively. Among studied molecules, **BPPP** contains maximum second-order polarizabilities (β_{tot}), contrarily, **BDMPP** consisting of minimum second-order polarizabilities (β_{tot}) as can be seen in Table 5. Urea is one of the prototypical compounds utilized in the investigation of the NLO properties of chemical systems and mostly utilized considering a threshold value for comparative purpose. The first hyperpolarizability (β_{tot}) of **BTFMP**, **BBPP** and **BPPP** is 4.0, 12.0 and 23.0 times larger respectively but **BDMPP** is 0.7 times less that of urea ($\beta = 43$) [54]. Hence, it is concluded that **BPPP** may be effective in NLO related device applications.

Molecular Electrostatic Potential (MEP) plots

Usually, the plot for total electron density in 3-D is termed molecular electrostatic potential (MEP) surface [55-56]. The MEP could be noteworthy descriptor for understanding the non-covalent interactions (NCIs) and reaction mechanism and MEP surface activity for both crystals. The relative reactivity of any compound in the context of electrophilic as well as nucleophilic attack can be explained by using different colors of an electrostatic potential plot [57-59]. The color scheme of any MEP map could be commenced from deep red to deep blue, in which blue color indicates positive potential whereas, red color indicates negative potential, so, the charge contribution could be systematic decreased order as red > orange > yellow > green > blue [60]. Consequently, it can be concluded that the red and yellow colored are best positions over MEP surface for attacking of electrophilic species while the blue colored are best positions over MEP surface for attacking of nucleophilic species. We displayed herein just MEP of **BPPP** and **BDMPP** as representative surfaces.

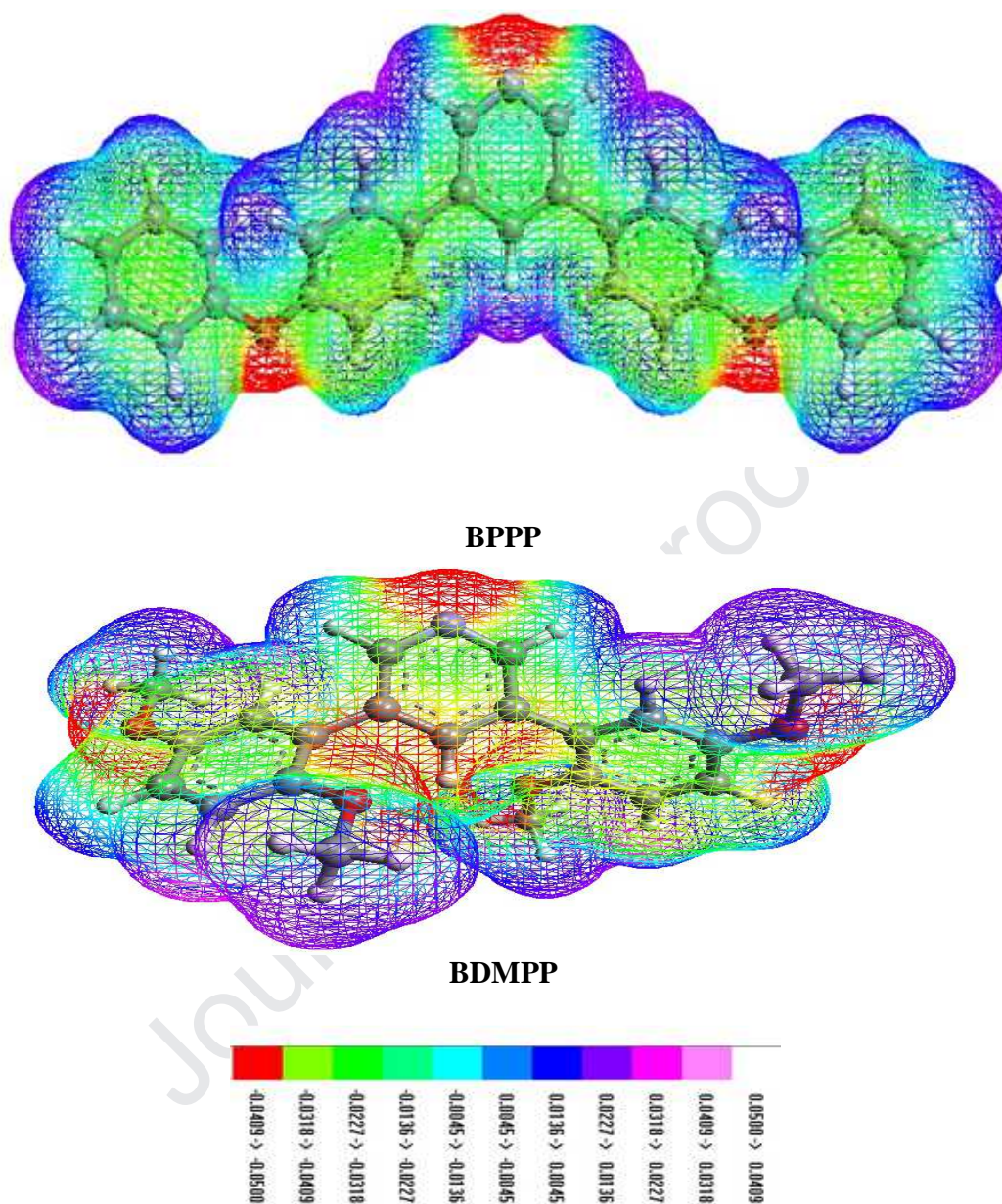


Figure 9: Molecular electrostatic potential surfaces for entitled derivatives.

Figure 9 pointed out that negative potential is disseminated over the oxygen atoms of phenoxy and methoxy moieties of **BPPP** and **BDMPP** respectively and nitrogen atoms of pyridine of both molecules. However, positive potential can be seen around the hydrogen atoms for BPPP and BDMPP as well as methyl group of methoxy moiety.

Conclusion

We synthesized four arylated pyridines derivatives with good yields by cross coupling Suzuki methodology for the first time. The structures of derivatives have been confirmed through ^1H NMR, ^{13}C NMR, ^{19}F NMR and FT-IR spectroscopic techniques. In addition, SC-XRD technique has been performed for **BPPP** and **BDMPP** which are confirmed as Orthorhombic, *Pnma* and Monoclinic, *P2₁/n* crystal systems with space groups respectively. The ground state geometric structures of **BTFMP**, **BBPP**, **BPPP** and **BDMPP** with spectroscopic FT-IR, FMOs, NBOs, MEP and NLO properties have been studied utilizing quantum chemical calculations. The DFT based geometric parameters are found in excellent concurrence to SC-XRD obtained data. NBO and FMO analysis provide a proof for the charge transfer interactions within the entitled molecules lead to nonlinear behaviour. Moreover, the hyperconjugative interactions affording stabilization to the chemical structures have been explained through second order perturbation energy analysis. The energy gap between HOMO and LUMO indicated that the structures of **BTFMP**, **BBPP**, **BPPP** and **BDMPP** can be efficiently polarized and appropriate to show NLO properties. Therefore, the values of the first hyperpolarizability of **BTFMP**, **BBPP** and **BPPP** are greater as compared to standard molecule. Due to unique electronic properties might open the method for **BTFMP**, **BBPP** and **BPPP** materials to be effective in NLO device applications. MEP surfaces explain the attacking of electrophilic and nucleophilic species on suitable positions of entitled molecules.

Conflict of interest

No conflicts declared.

Acknowledgments

Ataulpa A. C. Braga, (grants # 2011/07895-8, 2015/01491-3 and 2014/25770-6) is thankful to Fundação de Amparo à Pesquisa do Estado de São Paulo for financial support. AACB (grant 309715/2017-2) also thanks the Brazilian National Research Council (CNPq) for financial support and fellowships. This study was financed in part by the Coordenação de Aperfeiçoamento de Pessoal de Nível Superior - Brasil (CAPES) - Finance Code 001.

References

- [1] S. Reimann, P. Ehlers, S. Parpart, A. Surkus, A. Spannenberg, P. Langer, Site-selective synthesis of arylated pyridines by Suzuki-Miyaura reactions of 2,3,5,6-tetrachloropyridine, *Tetrahedron*, (71) (2015) 5371–5384.

- [2] G. Matolcsy, *Pesticide Chemistry*; Elsevier: Amsterdam, The Netherlands, 1988; p. 427.
- [3] G. Zhou, W. Y. Wong, X. Yang, New design tactics in OLEDs using functionalized 2-phenylpyridine-type cyclometalates of iridium (III) and platinum (II), *Chemistry*(6) (2011), 1706–1719.
- [4] A.K. Verma, R.R. Jha, R. Chaudhary, R.K. Tiwari, A.K. Danodia, 2-(1-Benzotriazolyl)pyridine: A robust bidentate ligand for the palladium-catalyzed CC (Suzuki, Heck, Fujiwara Moritani, Sonogashira), CN and CS coupling reactions. *Adv. Synth. Catal.* (355) (2013) 421–438.
- [5] B.A. Sweetman, H. Muller-Bunz, P.J. Guiry, Synthesis, resolution and racemisation studies of new tridentate ligands for asymmetric catalysis. *Tetrahedron Lett.* (46) (2005) 4643–4646.
- [6] (a) B. Corry, N.M. Smith, The role of thermodynamics and kinetics in ligand binding to G-quadruplex DNA, *Chem. Commun.*, 48(71) (2012) 8958–8960. (b) B. Tang, F. Yu, P. Li, L. Tong, X. Duan, T. Xie, X. Wang, A near-infrared neutral pH fluorescent probe for monitoring minor pH changes: imaging in living HepG2 and HL-7702 cells. *J. Am. Chem. Soc.*, 131(8) (2009) 3016–3023. (c) R. Karki, P. Thapa, H.Y. Yoo, T.M. Kadayat, P.H. Park, Y. Na, E. Lee, K.H. Jeon, W.J. Cho, H. Choi, Y. Kwon, Dihydroxylated 2, 4, 6-triphenyl pyridines: Synthesis, topoisomerase I and II inhibitory activity, cytotoxicity, and structure–activity relationship study. *Eur. J. Med. Chem.*, (49) (2012) 219–228. (d) M. Baumann, I.R. Baxendale, An overview of the synthetic routes to the best selling drugs containing 6-membered heterocycles. *Beilstein J. Org. Chem.*, 9(1) (2013) 2265–2319.
- [7] C. Doebelin, P. Wagner, F. Bihel, N. Humbert, C.A. Kenfack, Y. Mely, J.J. Bourguignon, M. Schmitt, Fully Regiocontrolled Polyarylation of Pyridine. *J. Org. Chem.* 79(3) (2014) 908–918.
- [8] K.K. Krishnan, S. Saranya, K.R. Rohit, G. Anilkumar, A novel zinc-catalyzed Suzuki-type cross-coupling reaction of aryl boronic acids with alkynyl bromides. *J. Catal.*, (372) (2019) 266–271.
- [9] G. Xiao, H. Min, Z. Zheng, G. Deng, Y. Liang, Copper-catalyzed three-component reaction of imidazo [1, 2-a] pyridine with elemental sulfur and arylboronic acid to

- produce sulfonylimidazo [1, 2-a] pyridines. *Chinese Chem. Lett.*, 29(9) (2018) 1363-1366.
- [10] F.Xu, W. Li, W. Shuai, L. Yang, Y. Bi, C. Ma, H. Yao, S. Xu, Z. Zhu, J. Xu, Design, synthesis and biological evaluation of pyridine-chalcone derivatives as novel microtubule-destabilizing agents, *Eur. J. Med. Chem.*, (173) (2019) 1-14.
- [11] D.K. Paluru, S. Dey, K.R. Chaudhari, M.V. Khedkar, B.M. Bhanage, V.K. Jain, Palladium (II) chalcogenolate complexes as catalysts for C-C cross-coupling and carbonylative Suzuki coupling reactions. *Tetrahedron Lett.*, 55(18) (2014) 2953-2956
- [12] Y. Riadi, S. Lazar, G. Guillaumet, Regioselective palladium-catalyzed Suzuki–Miyaura coupling reaction of 2, 4, 6-trihalogenopyrido [2, 3-d] pyrimidines. *C. R. Chim.*, 22(4) (2019) 294-298.
- [13] K.Tarade, S. Shinde, S. Sakate, C. Rode, Pyridine immobilised on magnetic silica as an efficient solid base catalyst for Knoevenagel condensation of furfural with acetyl acetone. *Catal. Commun.*, 124 (2019) 81-85.
- [14] S. M.Nobre, V.M. Cavalheiro, L.S. Duarte, Synthesis of brominated bisamides and their application to the suzuki coupling. *J. Mol. Str.*, (1171) (2018) 594-599.
- [15] T.Asako, W. Hayashi, K. Amaike, S. Suzuki, K. Itami, K. Muto, J. Yamaguchi, Synthesis of multiply arylated pyridines. *Tetrahedron*, 73(26) (2017) 3669-3676.
- [16] Y.S. Rozhkova, I.V. Plekhanova, A.A. Gorbunov, O.G. Stryapunina, E.N. Chulakov, V.P. Krasnov, M.A. Ezhikova, M.I. Kodess, P.A. Slepukhin, Y.V. Shklyaev, Synthesis of novel racemic 3, 4-dihydroferroceno [c] pyridines via the Ritter reaction. *Tetrahedron Lett.*, 60(11) (2019) 768-772.
- [17] C.Chai, S. Xu, J. Wang, F. Zhao, H. Xia, Y. Wang, Synthesis, photophysical properties and DFT studies of the pyridine-imidazole (PyIm) Cu (I) complexes: Impact of the pyridine ring functionalized by different substituents. *Inorg. Chim. Acta*, 488 (2019) 34-40.
- [18] D.K. Paluru, S. Dey, K.R. Chaudhari, M.V. Khedkar, B.M. Bhanage, V.K. Jain, Palladium (II) chalcogenolate complexes as catalysts for CC cross-coupling and carbonylative Suzuki coupling reactions. *Tetrahedron Lett.*, 55(18) (2014) 2953-2956.

-
- [19] M. Akram, M. Adeel, M. Khalid, M.N. Tahir, M.U. Khan, M.A. Asghar, M.A. Ullah, M. Iqbal, A combined experimental and computational study of 3-bromo-5-(2, 5-difluorophenyl) pyridine and 3, 5-bis (naphthalen-1-yl) pyridine: Insight into the synthesis, spectroscopic, single crystal XRD, electronic, nonlinear optical and biological properties. *J. Mol. Str.* 1160 (2018), 129-141.
- [20] A.A.Braga, G. Ujaque, F. Maseras, A DFT study of the full catalytic cycle of the Suzuki–Miyaura cross-coupling on a model system. *Organometallics*, 25(15) (2006) 3647-3658.
- [21] García-Melchor, M., Braga, A.A., Lledos, A., Ujaque, G. and Maseras, F., Computational perspective on Pd-catalyzed C–C cross-coupling reaction mechanisms. *Accounts Chem. Res.*, 46(11) (2013) 2626-2634.
- [22] A.A. Braga, N.H. Morgon, G. Ujaque, F. Maseras, Computational characterization of the role of the base in the Suzuki–Miyaura cross-coupling reaction. *J. Am. Chem. Soc.*, 127(25) (2005) 9298-9307.
- [23] M.J. Frisch, G.W. Trucks, H.B. Schlegel, G. Scuseria, M.A. Robb, J.R. Cheeseman, G. Scalmani, V. Barone, B. Mennucci, G. Petersson, H. Nakatsuji, M. Caricato, X. Li, H.P. Hratchian, A.F. Izmaylov, J. Bloino, G. Zheng, J.L. Sonnenberg, M. Hada, M. Ehara, K. Toyota, R. Fukuda, J. Hasegawa, M. Ishida, T. Nakajima, Y. Honda, O. Kitao, H. Nakai, T. Vreven, J.A. Montgomery, J.E. Peralta, F. Ogliaro, M. Bearpark, J.J. Heyd, B. E, K.N. Kudin, V.N. Staroverov, R. Kobayashi, J. Normand, K. Raghavachari, A. Rendell, J.C. Burant, S.S. Iyengar, J. Tomasi, M. Cossi, N. Rega, J.M. Millam, M. Klene, J.E. Knox, J.B. Cross, V. Bakken, C. Adamo, J. Jaramillo, R. Gomperts, R.E. Stratmann, O. Yazyev, A.J. Austin, R. Cammi, C. Pomelli, J.W. Ochterski, R.L. Martin, K. Morokuma, V.J. Zakrzewski, G.A. Voth, P. Salvador, J.J. Dannenberg, S. Dapprich, A.D. Daniels, O. Farkas, J.B. Foresman, J.V. Ortiz, J. Cioslowski, D.J. Fox, D. 0109, Revision D. 01, Gaussian, Inc., Wallingford, CT (2009).
- [24] F. Weinhold, E.D. Glendening, NBO 5.0 program manual: natural bond orbital analysis programs, Theoretical Chemistry Institute and Department of Chemistry, University of Wisconsin, Madison, WI 53706 (2001).
- [25] R. Dennington, T. Keith, J. Millam, GaussView, version 5, Semichem Inc., Shawnee Mission, KS (2009).

-
- [26] Avogadro, http://avogadro.cc/wiki/Main_Page.
- [27] N.M. O'boyle, A.L. Tenderholt, K.M. Langner, Cclib: a library for package-independent computational chemistry algorithms. *J. Comput. Chem.*, 29(5) (2008) 839-845.
- [28] ChemCraft, <http://www.chemcraftprog.com>.
- [29] A. Mahmood, T. Akram, E.B. de Lima, Syntheses, spectroscopic investigation and electronic properties of two sulfonamide derivatives: A combined experimental and quantum chemical approach. *J. Mol. Str.*, 1108 (2016) 496-507.
- [30] R.G. Parr, R.G. Pearson, Absolute hardness: companion parameter to absolute electronegativity. *J. Am. Chem. Soc.*, 105(26) (1983) 7512-7516.
- [31] Lesar, A. and Milošev, I., 2009. Density functional study of the corrosion inhibition properties of 1, 2, 4-triazole and its amino derivatives. *Chem. Phys. Lett.*, 483(4-6) (2009) 198-203.
- [32] Chattaraj, P.K., Sarkar, U. and Roy, D.R., Electrophilicity index. *Chem Rev.*, 106(6) (2006) 2065-2091.
- [33] R.G. Parr, L.V. Szentpály, S. Liu, Electrophilicity Index, *J. Am. Chem. Soc.*, 121(9) (1999) 1922–1924.
- [34] R.G. Parr, L.V. Szentpály, S. Liu, Electrophilicity Index, *J. Am. Chem. Soc.*, 121(9) (1999) 1922–1924.
- [35] T. Koopmans, Über die Zuordnung von Wellenfunktionen und Eigenwerten zu den Einzelnen Elektronen Eines Atoms, *Physica*, 1(1) (1934) 104–113.
- [36] P.K. Chattaraj, U. Sarkar, D.R. Roy, Electrophilicity index. *Chem. Rev.*, 106(6) (2006) 2065-2091.
- [37] Y. Sert, S. Sreenivasa, H. Doğan, N.R. Mohan, P.A. Suchetan, F. Uçun, Vibrational frequency analysis, FT-IR and Laser-Raman spectra, DFT studies on ethyl (2E)-2-cyano-3-(4-methoxyphenyl)-acrylate. *Spectrochim Acta A*, (130) (2014) 96-104.
- [38] M. Stolarczyk, I. Bryndal, A. Matera-Witkiewicz, T. Lis, K. Królewska-Golińska, M. Cieślak, J. Kaźmierczak-Barańska, J. Cieplik, , Synthesis, crystal structure and cytotoxic activity of novel 5-methyl-4-thiopyrimidine derivatives. *Acta Crystallogr C*, 74(10) (2018) 1138-1145.

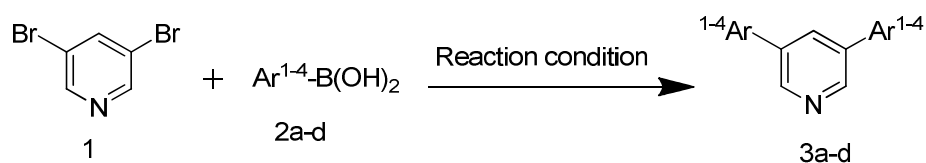
-
- [39] A.E.Reed, F. Weinhold, R. Weiss, J. Macheleid, Nature of the contact ion pair trichloromethyl-chloride ($\text{CCl}_3^+ \text{Cl}^-$). A theoretical study. *J. Phys. Chem-US*, 89(12) (1985) 2688-2694.
- [40] E.D.Glendenning, C.R. Landis, F. Weinhold, Natural bond orbital methods. *WIREs Comput Mol Sci*, 2(1) (2012) 1-42.
- [41] J.N. Liu, Z.R. Chen, S.F. Yuan, Study on the prediction of visible absorption maxima of azobenzene compounds. *J. Zhejiang Univ-Sc. B*, 6(6) (2005) 584-589.
- [42] R. S. Mulliken, "Electronic Population Analysis on LCAO-MO Molecular Wave Functions. I," *J. Chem. Phys.* 23(10) (1955) 1833-1840.
- [43] R.G. Parr, R.G. Pearson, Absolute hardness: companion parameter to absolute electronegativity. *J. Am. Chem. Soc.* 105(26) (1983) 7512-7516.
- [44] L. Li, C. Wu, Z. Wang, L. Zhao, Z. Li, C. Sun, T. Sun, Density functional theory (DFT) and natural bond orbital (NBO) study of vibrational spectra and intramolecular hydrogen bond interaction of l-ornithine-l-aspartate. *Spectrochim Acta A*, 136 (2015) 338-346.
- [45] M. Stolarczyk, I. Bryndal, A. Matera-Witkiewicz, T. Lis, K. Królewska-Golińska, M. Cieślak, J. Kaźmierczak-Barańska, J. Cieplik, , Synthesis, crystal structure and cytotoxic activity of novel 5-methyl-4-thiopyrimidine derivatives. *Acta Crystallogr C*, 74(10) (2018) 1138-1145.
- [46] Z.A.Li, H. Kim, S.H. Chi, J.M. Hales, S.H. Jang, J.W. Perry, A.K.Y. Jen, Effects of counterions with multiple charges on the linear and nonlinear optical properties of polymethine salts. *Chem. Mater.*, 28(9) (2016) 3115-3121.
- [47] D.Recatalá, R. Llusar, A. Barlow, G. Wang, M. Samoc, M.G. Humphrey, A.L. Guschin, Synthesis and optical power limiting properties of heteroleptic Mo 3 S 7 clusters. *Dalton Trans.*, 44(29) (2015) 13163-13172.
- [48] J. Schmitt, V. Heitz, A. Sour, F. Bolze, H. Ftouni, J.F. Nicoud, L. Flamigni, B. Ventura, Diketopyrrolopyrrole-Porphyrin Conjugates with High Two-Photon Absorption and Singlet Oxygen Generation for Two-Photon Photodynamic Therapy. *Angew. Chem. Inter. Edi.*, 54(1) (2015) 169-173.

-
- [49] R. Medishetty, J.K. Zaręba, D. Mayer, M. Samoć, R.A. Fischer, Nonlinear optical properties, upconversion and lasing in metal–organic frameworks. *Chemical Society Rev.*, 46(16) (2007) 4976-5004.
- [50] K.B. Manjunatha, R. Rajarao, G. Umesh, B.R. Bhat, P. Poornesh, Optical nonlinearity, limiting and switching characteristics of novel ruthenium metal-organic complex. *Opt. Mater.* 72 (2017) 513-517.
- [51] A.J. Almosawe, H.L. Saadon, Nonlinear optical and optical limiting properties of new structures of organic nonlinear optical materials for photonic applications. *Chin. Opt. Lett.* 11(4) (2013) 041902.
- [52] X. Zhan, J. Zhang, S. Tang, Y. Lin, M. Zhao, J. Yang, H.L. Zhang, Q. Peng, G. Yu, Z. Li, Pyrene fused perylene diimides: synthesis, characterization and applications in organic field-effect transistors and optical limiting with high performance. *Chem. Comm.* 51(33) (2015) 7156-7159.
- [53] R.J. Durand, S. Achelle, S. Gauthier, N. Cabon, M. Ducamp, S. Kahlal, J.Y. Saillard, A. Barsella, F. Robin-Le Guen, Incorporation of a ferrocene unit in the π -conjugated structure of donor-linker-acceptor (D- π -A) chromophores for nonlinear optics (NLO). *Dyes Pigments*, 155 (2018) 68-74.
- [54] P.N. Prasad, D.J. Williams, Introduction to nonlinear optical effects in molecules and polymers, Wiley New York etc.1991.
- [55] N. Okulik, A.H. Jubert, Theoretical analysis of the reactive sites of non-steroidal anti-inflammatory drugs. *Internet Elec. J. Mol. Design*, 4(1) (2005) 17-30.
- [56] Muthu, S. and Prabhakaran, A., Vibrational spectroscopic study and NBO analysis on tranexamic acid using DFT method. *Spectrochim. Acta A*, 129 (2014) 184-192.
- [57] E.Scrocco, J. Tomasi, Electronic molecular structure, reactivity and intermolecular forces: an euristic interpretation by means of electrostatic molecular potentials. *Adv.Quant. Chem.*11 (1978) 115-193. Academic Press.
- [58] F.J. Luque, J.M. López, M. Orozco, Perspective on “Electrostatic interactions of a solute with a continuum. A direct utilization of ab initio molecular potentials for the prevision of solvent effects”. *Theor. Chem. Acc.*, 103(3-4) (2000) 343-345.

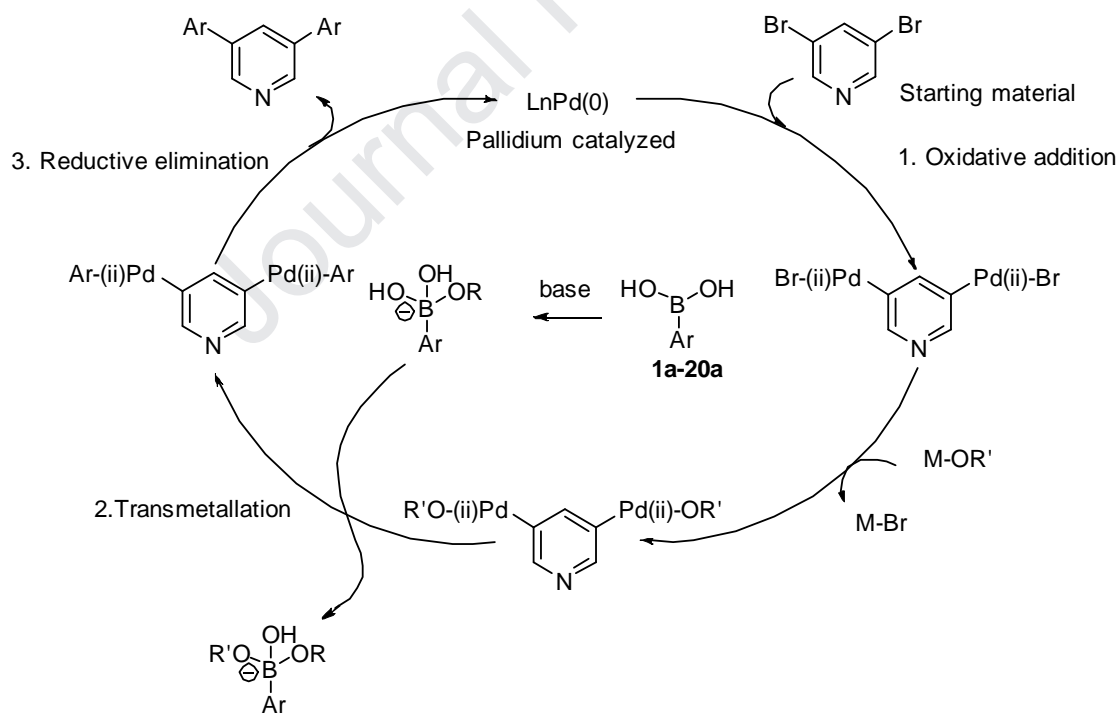
-
- [59] J. S. Murray, K. Sen, *Molecular electrostatic potentials: concepts and applications*, Elsevier 1996.
- [60] G. Mahalakshmi, V. Balachandran, NBO, HOMO, LUMO analysis and vibrational spectra (FTIR and FT Raman) of 1-Amino 4-methylpiperazine using ab initio HF and DFT methods. *Spectrochimica Acta Part A: Molecular and Biomolecular Spectroscopy*, (135) (2015) , 321-334.

Journal Pre-proof

Journal Pre-proof



Product	Ar ¹⁻⁴ -B(OH) ₂	Yield %
3a-BTFMP		87%
3b-BBPP		85%
3c-BPPP		85%
3d-BDMPP		92%



Scheme 1: Synthesis of derivatives of arylated pyridines.

Highlights

- The arylated pyridines derivatives: **BTFMP**, **BBPP**, **BPPP** and **BDMPP** were synthesized
- The said derivatives were characterized by spectroscopic techniques
- The SC-XRD was performed for **BPPP** and **BDMPP**
- DFT based analysis were performed for **BTFMP**, **BBPP**, **BPPP** and **BDMPP**
- A good agreement is obtained between DFT and experimental findings

Benefiting Author Statement

Dear Editor,

Journal of Molecular Structure

I am pleased to submit a manuscript entitled as “*Highly Efficient one Pot Palladium-Catalyzed Synthesis of 3,5-bis (arylated) pyridines: Comparative Experimental and DFT Studies*” to be considered for publication in your esteemed journal.

We feel that this manuscript is relevant for publication in *Journal of Saudi Chemical Society*, because of the main interest of the journal is in novel findings by experimental and density functional theory (DFT) analysis of compounds. Herein, we reported the arylated pyridines derivatives: 3, 5-bis (4-(trifluoromethoxy) phenyl) pyridine (**BTFMP**), 3,5-bis(4-bromophenyl)pyridine (**BBPP**), 3,5-bis(4-phenoxyphenyl)pyridine (**BPPP**) and 3,5-bis(2,5-dimethoxyphenyl)pyridine (**BDMPP**) by cross coupling Suzuki methodology for the first time. All derivatives have been characterized through ¹H NMR, ¹³CNMR, ¹⁹F NMR and FT-IR spectroscopic techniques. Two compounds (**BPPP**) and (**BDMPP**) exist in the form of crystals among studied compounds. Therefore, SC-XRD has been performed for **BPPP** and **BDMPP**. In addition, computational studies using density functional theory (DFT) have been carried out in order to compare the DFT based data with the experimental findings. To the best of our knowledge, no similar study regarding the investigated molecules has been reported so far. Furthermore, I certify that this manuscript, or any part of it, has not been published and will not be submitted elsewhere for publication.

I will be looking forward for your favorable consideration.

Warm Regards

Most sincerely,

Dr. Muhammad Adeel

Assistant Professor,

Institute of Chemical Sciences, Gomal University

Dear Ismail Khan, Pakistan

Email: madeel@gu.edu.pk

Journal Pre-proof

Declaration of interests

The authors declare that they have no known competing financial interests or personal relationships that could have appeared to influence the work reported in this paper.

The authors declare the following financial interests/personal relationships which may be considered as potential competing interests:

Journal Pre-proof